# Estimation of pasture productivity in Mongolian grasslands: Field survey and Model simulation

モンゴル草原における牧草生産力の推定：

現地調査およびモデルシミュレーション

by

**Tserenpurev BAT-OYUN**

A thesis submitted to the United Graduate School of Agricultural Sciences, Tottori University

In partial fulfillment of the requirements
for the degree of

**DOCTOR OF PHILOSOPHY**

in

**BIOENVIRONMENTAL SCIENSE**

September 2011

# Acknowledgements

I wish to thank many individuals who have assisted me with their knowledge or friendship during this research, without their contributions this research would not been accomplished.

First of all, I am deeply grateful to my supervisors Prof. Masato Shinoda and Assoc. Prof. Mitsuru Tsubo for their guidance, constructive discussion and expert advice during my PhD study. I am highly indebted to Prof. Masato Shinoda and Assoc. Prof. Mitsuru Tsubo for their invaluable support. I also wish to express my deepest thanks to Prof. Masato Shinoda and Prof. Atsushi Tsunekawa, who gave me the opportunity to pursue higher education at The United Graduate School of Agricultural Sciences, Tottori University.

I also would like to thank my co-supervisor, Assoc. Prof. Ibaraki Yasuomi and Assoc. Prof. Reiji Kimura for their suggestion comments on my study.

I wish to express my sincere thanks to the members of the Dissertation Committee of The United Graduate School of Agricultural Sciences, Tottori University for the comments and suggestion on this thesis.

I would like to extend my profound gratitude to the Japanese government to support me Monbukagakusho: MEXT scholarship and Global Center of Excellence for Dryland Science Foundation.

I would like to thank to colleagues of Agrometeorological division of the Institute of Meteorology and Hydrology for providing the required data and their great help.

Special thanks to Prof. Tomoko Nakano for her suggestion and comments on my study.

My sincere thanks go to all my colleagues, friends, and students for their suggestion, assistance, friendship, and support.

Also, I would like to thank the staff at Arid Land Research Center, Tottori University for their support and assistance.

I am deeply grateful to my parents, my husband PUREVDORJ and my lovely daughter AMINA, my brothers and sisters, for their infinite love and great support.

Thank you very much for all of you!

**Author:** Tserenpurev BAT-OYUN

# TABLE OF CONTENTS

## Chapter 4: Effects of water and temperature stresses on radiation use efficiency



## Chapter 5: Estimation of pasture productivity in Mongolian grasslands

## Chapter 6

# LIST OF ABBREVIATIONS

| | |
|---|---|
| AGB | Aboveground biomass |
| ANPP | Aboveground net primary productivity |
| APAR | Absorbed photosynthetically active radiation |
| BGB | Belowground biomass |
| *fAPAR* | Fraction of absorbed photosynthetically active radiation |
| *fIPAR* | Fraction of intercepted photosynthetically active radiation |
| GPP | Gross primary production |
| IPAR | Intercepted photosynthetically active radiation |
| LAI | Leaf area index |
| NDVI | Normalized difference vegetation index |
| NIR | Near infrared radiation |
| NPP | Net primary productivity |
| PAR | Photosynthetically active radiation |
| PAR/SR | Ratio of PAR to SR |
| PEM | Production efficiency model |
| RUE | Radiation use efficiency |
| SimR | Simple ratio |
| SR | Global solar radiation |
| SWC | Soil water content |

# LIST OF FIGURES

# LIST OF TABLES

# CHAPTER 1

# General Introduction

## 1. 1 Background

Mongolia is a landlocked country in the eastern part of the Eurasian continent. It has an average altitude of 1580 m above sea level, is surrounded by high mountains, and is situated far from oceanic influences. These geographical characteristics have led to a continental and dry climate characterized by a long-lasting cold winter, hot and dry summer, low precipitation, and high diurnal and seasonal temperature fluctuations. The climate in Mongolia is related to the existence of two types of meteorological disasters; drought and *dzud* (Appendix A on page 78) which have dramatic impacts on livestock survival. The average annual air temperature in Mongolia is 0.7ºC (Batima, 2006), compared with +8.5ºC in the warmest regions of the Gobi and south Altai deserts, and –7.8ºC in the coldest region of the Darkhad depression. A remarkable feature of this climate is the number of clear, sunny days (between 220 and 260 per year), which results in high annual solar radiation. Precipitation increases with altitude and latitude, ranging from less than 100 mm/yr in low-lying desert areas to about 400 mm/yr in the north of the country. Pasture productivity decreases from north to south according to the distribution of precipitation. Bolortsetseg *et al*. (2002) analyzed 40 years of animal-available aboveground biomass (AGB) (located above the 1 cm height of grasses from the ground surface) data over 60 sites in different vegetation zones within Mongolia. The average

peak standing biomass was 59 g/m$^2$ in forest steppe, 30 g/m$^2$ in steppe, 22 g/m$^2$ in desert steppe, and 17 g/m$^2$ in the Altai Mountains and desert. The yearly maximum of pasture biomass has declined from 20% to 30% during the past 40 years.

Pastoral animal husbandry plays a key role in the Mongolian economy, amounting to 20% of Gross Domestic Product, and 35% of the population is reliant on this activity for their livelihood (Statistical Book of Mongolia, 2009). Livestock production is strongly dependent on the productivity of natural grasslands, which cover 80% of the country (Batima and Dagvadorj, 2000). Grassland productivity is regulated by many factors, including precipitation, temperature, solar radiation, soil nutrient availability, and grassland utilization and management. Among these, water stress is the most critical limiting factor determining the efficiency of plant radiation utilization and vegetation productivity in drylands, because of the low precipitation and high evapotranspiration at these localities (Noy-Meir, 1973; Munkhtsetseg *et al*., 2007; Li *et al*., 2008; Nakano *et al*., 2008). Water deficiency in plants restricts their potential carbon assimilation by affecting photosynthetic processes through decreased stomatal conductance, which not only decreases photosynthesis but also slows respiration and transpiration per unit area (Day *et al*., 1981).

The large area and geography of Mongolia make it difficult to monitor vegetation conditions using field measurements at specific locations; consequently, it is difficult to gain a comprehensive understanding of how grasslands respond to factors such as climate, grazing, fire, and management. Modeling is essential to improve our understanding of the complex dynamics of ecosystems such as grasslands. A number of models have been developed to simulate the productivity of different ecosystems. Those that focus on production efficiency are the simplest and most commonly used methods for analyzing and modeling plant growth using ground and satellite remote-sensing-based data

(Monteith, 1972, 1977). In Mongolia, there has been limited progress in estimating and modeling the carbon cycle of grassland ecosystems, and substantial uncertainties remain regarding net primary productivity (NPP) estimations. Given this background, continuous monitoring and modeling of grassland productivity would be valuable information for herders and decision-makers to assist pasture management.

## 1.2 Production Efficiency Models

Production Efficiency Models (PEMs) are commonly used to estimate NPP at the local and global scale (Kumar and Monteith, 1981; Prince, 1991a). In the present study, a PEM with quantified parameters has been used to simulate pasture productivity in Mongolian steppe. In the model, above-ground NPP (ANPP) is sensitive to resources, such as solar radiation (which is location-dependent), and to resource regulators (i.e., environmental conditions) (Figure 1.1). Detailed explanations of key model parameters are given below.

### 1.2.1 Net primary productivity

Net primary productivity is a key output parameter of the PEM, and is used widely as an indicator of the accumulation of atmospheric $CO_2$ in terrestrial ecosystems. It also plays an important role in studying the global carbon cycle, carbon sources and sinks, and the spatial and temporal distribution of $CO_2$. NPP represents the net new carbon stored as biomass in the stems, leaves, and roots of plants. It constitutes the difference between carbon assimilated during photosynthesis by plant leaves and carbon consumption through respiration by the stems, leaves, and roots (Cooper, 1975; Coupland, 1979; Jordan, 1981; Roberts *et al*., 1985). NPP is therefore a quantitative measure of plant growth and carbon

uptake, and it is a sum of two components: ANPP and below-ground NPP (BNPP). ANPP is the amount of carbohydrates allocated to above-ground parts of the vegetation minus respiration. BNPP, which is one of the most poorly understood attributes of terrestrial ecosystems, is the rate of partitioning of energy to below-ground parts. Over any given period, NPP equals the change in plant mass ($\Delta W$) plus any losses through death (L) from both above and below ground parts (Roberts *et al.*, 1985):

$$NPP = \Delta W + L \tag{1.1}$$

In terms of carbon exchange, NPP can be defined as follows:

$$NPP = GPP - R_a \tag{1.2}$$

where GPP is gross primary productivity and $R_a$ is autotrophic respiration.

In the PEM used here, the NPP component is based on the concept of radiation use efficiency (RUE), described by Monteith (1972, 1977) as follows:

$$ANPP(AGB) = SR \cdot PAR/SR \cdot fIPAR(fAPAR) \cdot RUE \tag{1.3}$$

where SR is global solar radiation, PAR/SR is the ratio of photosynthetically active radiation (PAR) to SR, and *fIPAR* (*fAPAR*) is the fraction of intercepted PAR (fraction of absorbed PAR). Above-ground NPP was assumed to be an approximation of above-ground biomass (AGB) for the grassland ecosystem.

In the proposed model, SR was initially converted into PAR using a pre-determined PAR/SR ratio (Chapter 3). Normalized difference vegetation index (NDVI) data were then used to estimate *fIPAR* as a means of obtaining total-intercepted PAR

(IPAR) or absorbed PAR (APAR) (Chapter 4). RUE was quantified based on field-measured AGB and IPAR (Chapter 4). Finally, ANPP (AGB) was estimated by applying observed and quantified parameters to the model (Chapter 5).

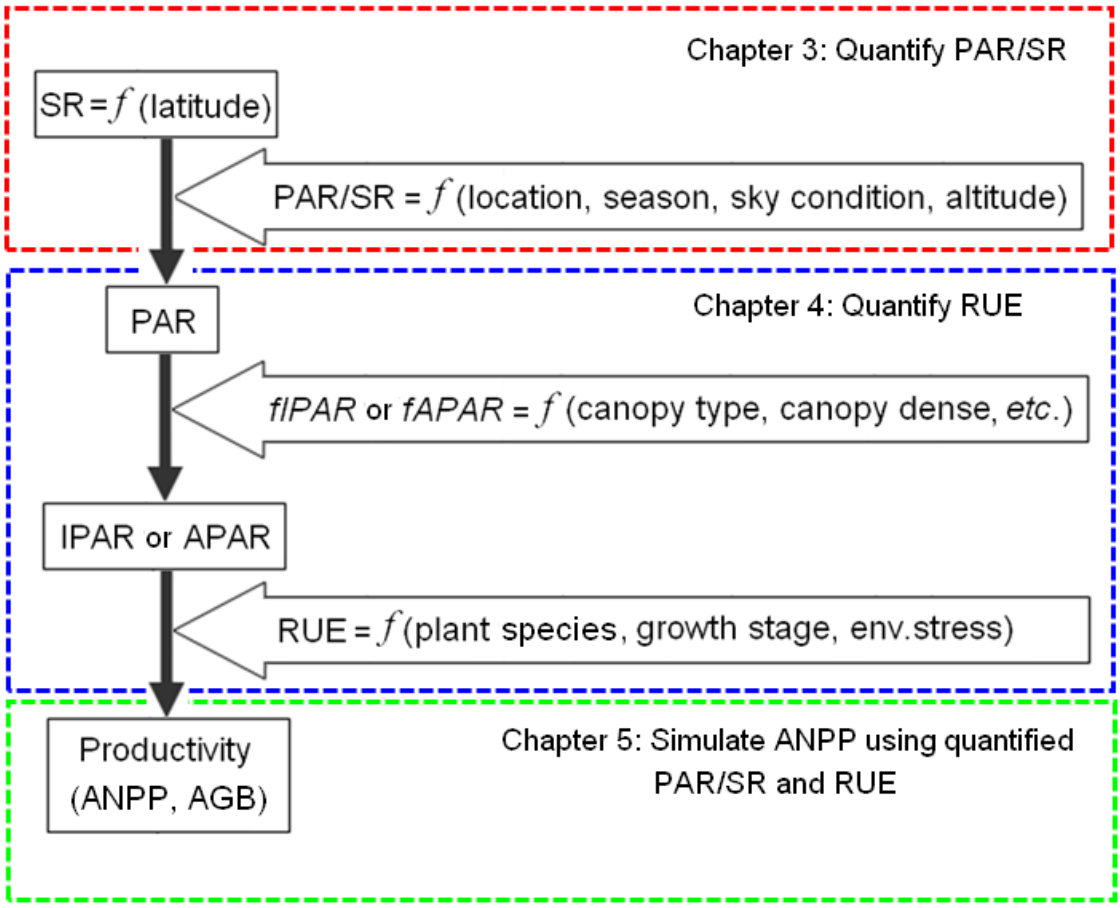


**Figure 1.1** General flow from solar energy to plant productivity. The flowchart gives the general sequence of present study.

### 1.2.2 Global solar radiation and PAR

Global solar radiation (SR) is the primary energy source for many processes in the natural environment. It is dependent on the solar angle, which is determined by the daily rotation of the Earth and its orbit around the sun (Sinclair and Gardner, 1998). Radiation attenuation subsequently occurs in the atmosphere as a result of molecular and aerosol

scattering, and by ozone, water vapor, and other atmospheric gas absorption (Monteith and Unsworth, 1990). PAR is a portion of the solar spectrum ranging from 0.4 μm (deep violet) to 0.7 μm (dark red), which plants use for the process of photosynthesis. A worldwide routine network for the measurements of PAR has yet to be established, but SR data are widely collected by weather stations (Papaioannou *et al*., 1993). Therefore, accurate determination of PAR/SR is an efficient way of obtaining a key model input parameter of PAR based on SR, which occurs under similar or representative conditions. PAR/SR varies according to location (Tsubo and Walker, 2005), season (Udo and Aro, 1999), sky conditions (Rao, 1984), and altitude (Wang *et al*., 2007) (Figure 1.1).

### 1.2.3 Intercepted PAR or Absorbed PAR

Only some portion of incident PAR can be intercepted or absorbed by vegetation; the remaining part is either scattered back into the atmosphere or transmitted to the soil. IPAR or APAR is an important parameter for determining plant growth because it has a linear relationship with dry matter (Monteith, 1972). IPAR is the amount of PAR captured by canopy layers, as the incident PAR at the top of the canopy travels through these layers to the ground. APAR is the amount of PAR actually absorbed by canopy layers. It takes into account PAR reflected off the canopy top back into the atmosphere and PAR reflected off the soil or background material into the canopy. The difference between IPAR and APAR depends on canopy closure (dense or sparse). If a canopy has full coverage of green leaves, IPAR may be a good approximation of APAR because healthy green leaves reflect little PAR. IPAR or APAR can be estimated from *fIPAR* or *fAPAR* and total incident PAR. *fIPAR* or *fAPAR* is therefore one of the key quantities in models assessing vegetation primary productivity. Variations in *fIPAR* or *fAPAR* depend on canopy type, density, and biochemical composition, as well as background reflectance (Figure 1.1). The *fIPAR* or

*fAPAR* is often calculated as a linear function of the remote-sensing-based NDVI (Asrar *et al*., 1984).

### 1.2.4 Radiation use efficiency

Accurate estimation of RUE is essential in modeling plant productivity. RUE is another important parameter in the PEM because it is an indicator of the plant conversion efficiency of the IPAR or APAR into organic dry matter (carbon) through photosynthesis. The value of RUE varies widely depending on plant species, growth stage, and environmental conditions (Figure 1.1), and representative values must be determined for each distinct vegetation type or biome. The PEM incorporates factors that affect RUE, including temperature and water stress.

## 1.3 STUDY OBJECTIVES

The main objectives of this thesis were to quantify model input parameters (PAR/SR and RUE) and to examine the suitability of the parameterized PEM in estimating pasture productivity in different vegetation zones of Mongolia. Specific objectives of the research were given below.

- To assess the effects of precipitation and grazing on AGB (Chapter 2).
- To quantify PAR/SR and to investigate its dependence on sky condition and atmospheric water vapor condition in steppe grassland habitats (Chapter 3).
- To investigate the effects of water and temperature stress on vegetation growth and radiation interception in grasslands, to examine the relationship between *fIPAR* and NDVI, and to quantify RUE for steppe grassland (Chapter 4).
- To perform a sensitivity analysis of the effect of climate on ANPP and to test model simulations with quantified parameters for four sites in different vegetation zones (Chapter 5).

# CHAPTER 2

## Effects of precipitation and grazing on pasture productivity

## 2.1 Introduction

Mongolia has large areas of open grassland that are grazed all year round (Appendix B on page 79). It is important to study grassland productivity and its dependence on climatic and grazing conditions because of the implications this has for livestock production. Drought has become widespread in the Northern Hemisphere since the mid-1950s, especially over northern Eurasia (Dai *et al*., 2004). In Mongolia, drought frequency (i.e., the number of dry days) has increased and become widespread since the mid-1960s (Natsagdorj, 2009), resulting in a substantial decrease in grassland productivity (Miyazaki *et al*., 2004; Munkhtsetseg *et al*., 2007) and changing phenology (Kondoh *et al*., 2005; Shinoda *et al*., 2007). In addition, during the past several decades the intensity of precipitation and the frequency of extreme events have increased worldwide (Easterling *et al*., 2000; Weltzin *et al*., 2003), and grasslands have been greatly affected (Knapp and Smith, 2001; Fay *et al*., 2003; Fang *et al*., 2005; Nippert *et al*., 2006). For most ecosystems, especially those in arid and semi-arid environments, precipitation is the

predominant climatic factor controlling ecosystem processes (Boutton *et al*., 1988; Gunin *et al*., 1999).

Zolotokrilin (2001) concluded that precipitation of 0.1–6.0 mm/day could be effectively used by plant growth in the southern Russia and Kazakhstan. Previous studies reported that low precipitation (<5 mm) did not contribute to soil water content (SWC) at 10 cm depth in a Mongolian grassland (Nakano *et al*., 2008; Shinoda *et al*., 2010b). The objectives of this chapter were thus to improve our understanding of the responses of grassland productivity to changes in precipitation parameters (amount, event size) by focusing on three main vegetation zones, and to explore the effect of grazing on plant parameters by using ground-based measurements at Bayan Unjuul.

## 2.2 Materials and methods

Fifteen sites were selected within the major vegetation zones of desert steppe, steppe, and forest steppe (five sites in each zone) (Table 2.1). AGB, measured on 14 August (a period to reach its peak) in 1986–2005 was obtained from Mongolian Institute of Meteorology and Hydrology (IMH). The IMH have measured animal-available AGB of fenced pasture in four 1 $m^2$ plots at each of the study sites between 1986 and 2005. In addition, daily precipitation was obtained from the IMH during the growth period (1 May–13 August) of 1986–2005, which have been categorized into three classes of precipitation event: small (≤5 mm), medium (5.1–10 mm), and large (≥10.1 mm).

AGB and plant height were measured in “no-grazing plots” (i.e., fenced enclosures used to prevent livestock grazing since June 2004 [hereinafter referred to as non-grazing site (NG site)]) and “grazing plots” (unfenced areas) at Bayan Unjuul, in July of 2005–2007. The experimental layout was a fully randomized design, consisting of two treatments (the no-grazing and grazing plots) with four replicates (quadrats).

**Table 2.1** Study sites with location and elevation.

| Natural zone | Site name | Latitude (°N) | Longitude (°E) | Altitude (m) |
|---|---|---|---|---|
| Desert steppe | Gurvantes | 43.20 | 101.00 | 1726 |
| | Mandalgobi | 45.75 | 106.27 | 1393 |
| | Nogoonnuur | 49.53 | 89.79 | 1480 |
| | Tsogt-Ovoo | 44.42 | 105.32 | 1299 |
| | Zereg | 47.13 | 92.82 | 1152 |
| Steppe | Bayandelger | 45.73 | 112.35 | 1108 |
| | Choibalsan | 48.07 | 114.52 | 759 |
| | Khujirt | 46.9 | 102.77 | 1662 |
| | Ulaangom | 49.97 | 92.07 | 939 |
| | Underhaan | 47.32 | 110.67 | 1033 |
| Forest steppe | Bulgan | 48.82 | 103.52 | 1209 |
| | Dashbalbar | 49.55 | 114.38 | 705 |
| | Erdenemandal | 48.53 | 101.38 | 1509 |
| | Kharhorin | 47.2 | 102.79 | 1430 |
| | Tarialan | 49.62 | 101.98 | 1236 |

# 2.3 Results and discussion

## 2.3.1 Characteristics of the precipitation parameters

The long-term average of growing season precipitation (1 May–13 August) varied greatly from region to region from 1986–2005. It was greater in forest steppe sites (208 mm) than in steppe (149 mm) and desert steppe sites (69 mm). Small precipitation events were most frequent, accounting for 71%–78% of the total number of events, while medium and large precipitation events accounted for just 14%–15% and 8%–14%, respectively, in the three zones (Figure 2.1a–c). Sala and Lauenroth (1982) reported similar findings for a study in north-central Colorado, USA, where small precipitation events (≤5 mm) accounted for 67% of the total rainfall.

The present results show weak increasing trends in the number of days with ≤5 mm, 5.1–10 mm, and ≥10.1 mm of precipitation in desert steppe. Conversely, there is decreasing trends observed at steppe and forest steppe (Figure 2.1d-f); among these decreases in number of days with 5.1–10 mm of precipitation at steppe sites, and number of days with 5.1–10 mm and ≥ 10.1 mm of precipitation at forest steppe sites were statistically significant ($p < 0.05$). A significant decreasing trend in soil moisture is also evident in the forest steppe zone of Mongolia due to lower precipitation and higher evapotranspiration (Nandintsetseg and Shinoda, 2010).

### 2.3.2 Precipitation effect on aboveground biomass

In the previous section, a latitudinal gradient in precipitation was found, decreasing from north to south. This gradient was consistent with AGB: the highest AGB occurred in forest steppe (68.8 g/m$^2$), whereas lower AGB was recorded in steppe (30.4 g/m$^2$) and desert steppe (9.7 g/m$^2$). Table 2.2 shows the relationship between AGB and monthly cumulative precipitation during the growing season for each site and vegetation zone (data from all five sites have been combined). Cumulative precipitation had the strongest impact on AGB for all vegetation zones (Table 2.2; Figure 2.2). However, in several cases, site-by-site correlation revealed that precipitation had the greatest impact on AGB during individual months (Table 2.2): precipitation in July had the highest potential to enhance AGB for desert steppe and steppe zones. This finding is consistent with previous studies conducted in Mongolian desert steppe (Munkhtsetseg *et al.*, 2007) and steppe sites (Miyazaki *et al.*, 2004). However, precipitation during June had the greatest effect on AGB in forest steppe zone. There was no relationship between AGB in August and precipitation in May for steppe and forest steppe zones, which are colder than desert steppe (Table 2.2).

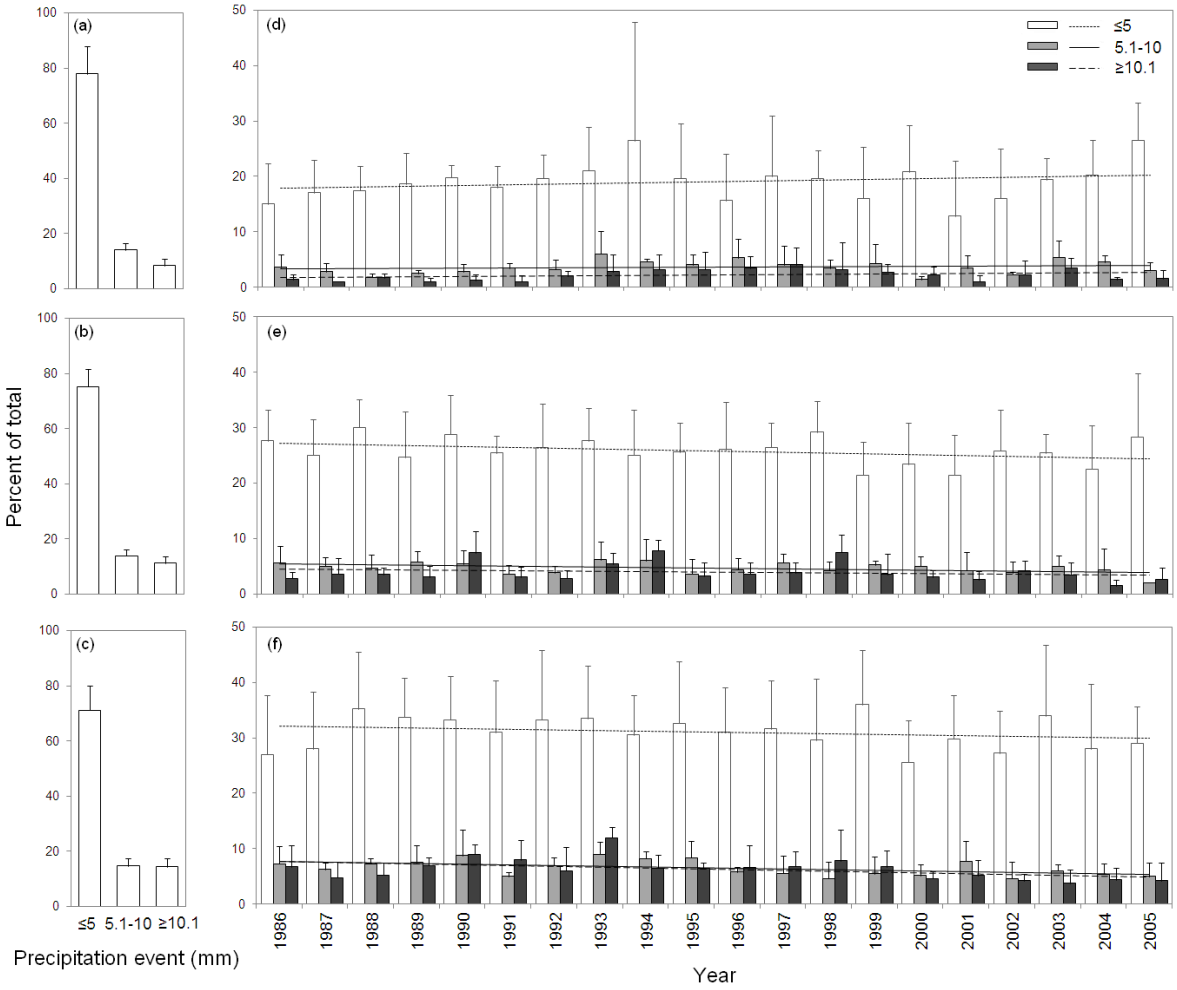


**Figure 2.1** Percentage of precipitation events with different sizes ($\leq$5 mm, 5.1–10 mm, and $\geq$10.1 mm) during the growth period (1 May–13 August) in 1986–2005 averaged over five sites for (a) desert steppe, (b) steppe and (c) forest steppe; and time series of number of days with different precipitation sizes during the growth period in 1986–2005 averaged over five sites for (d) desert steppe, (e) steppe and (f) forest steppe.

**Table 2.2** Correlations between AGB (on 14 August) and monthly, cumulative precipitation (1 May–13 August) during 1986–2005 for each site and for data of five sites combined in each vegetation zones.

| Natural zone | Station name | May | June | July | 1 Aug-13 Aug | 1 May-13 Aug |
|---|---|---|---|---|---|---|
| Desert steppe | Gurvantes | 0.59 * | 0.25 ns | 0.32 ns | 0.61 ** | 0.78 *** |
| | Mandalgovi | 0.03 ns | 0.13 ns | 0.71 ** | 0.20 ns | 0.65 ** |
| | Nogoonnuur | 0.45 ns | 0.51 ns | 0.22 ns | -0.02 ns | 0.62 * |
| | Tsogt-Ovoo | -0.25 ns | 0.19 ns | 0.66 ** | 0.57 * | 0.67 ** |
| | Zereg | 0.52 ns | 0.27 ns | 0.39 ns | 0.13 ns | 0.70 * |
| | **Over five stations** | **0.24 *** | **0.34 **** | **0.57 ***** | **0.36 ***** | **0.72 ***** |
| Steppe | Bayandelger | -0.36 ns | 0.56 * | 0.72 ** | 0.34 ns | 0.64 * |
| | Choibalsan | -0.40 ns | 0.59 * | 0.41 ns | 0.40 ns | 0.46 ns |
| | Khujirt | 0.25 ns | 0.40 ns | 0.32 ns | 0.29 ns | 0.54 * |
| | Ulaangom | 0.02 ns | -0.06 ns | 0.67 * | 0.14 ns | 0.55 ns |
| | Underhaan | -0.51 ns | -0.03 ns | 0.46 ns | 0.62 * | 0.60 * |
| | **Over five stations** | **-0.15 ns** | **0.27 *** | **0.45 ***** | **0.44 ***** | **0.49 ***** |
| Forest steppe | Bulgan | -0.08 ns | 0.43 ns | 0.11 ns | 0.18 ns | 0.33 ns |
| | Dashbalbar | 0.09 ns | 0.52 * | 0.39 ns | 0.29 ns | 0.48 ns |
| | Erdenemandal | -0.12 ns | 0.64 *** | 0.33 ns | 0.14 ns | 0.53 * |
| | Kharhorin | 0.38 ns | 0.86 ** | 0.10 ns | -0.03 ns | 0.53 ns |
| | Tarialan | 0.10 ns | 0.37 * | 0.28 ns | 0.44 ns | 0.68 ** |
| | **Over five stations** | **-0.02 ns** | **0.40 ***** | **0.27 *** | **0.28 *** | **0.46 ***** |

* Correlation is significant at the 0.05 level, ** Correlation is significant at the 0.01 level, *** Correlation is significant at the 0.001 level, ns Correlation is not significant.

The relationship between AGB and the size of precipitation events was examined to improve our understanding of how precipitation size affects on grass growth. Table 2.3 lists the correlation coefficient between AGB and the number of days with different sizes of precipitation events for each site and for all three zones (data from the five sites have again been combined). In the desert steppe zone, precipitation is strongly correlated with AGB, independent of event size (Table 2.3). This result indicates that plants in desert steppe habitats are capable of responding rapidly to small, frequent precipitation events (≤5 mm). Similarly, Fang *et al*. (2005) demonstrated that more frequent and less intense, evenly distributed, precipitation patterns promote plant growth in temperate grasslands of China. However, for steppe and forest steppe, it is likely that less frequent and large

precipitation events are typically required for high productivity (Table 2.3). This suggests that large precipitation events, which infiltrate deeper into the soil layers, may be necessary for the grasslands in steppe and forest steppe sites to obtain high AGB. Precipitation events of 15–30 mm also accounted for most of the variability in the productivity of short-grass steppe in North America (Lauenroth and Sala, 1992).

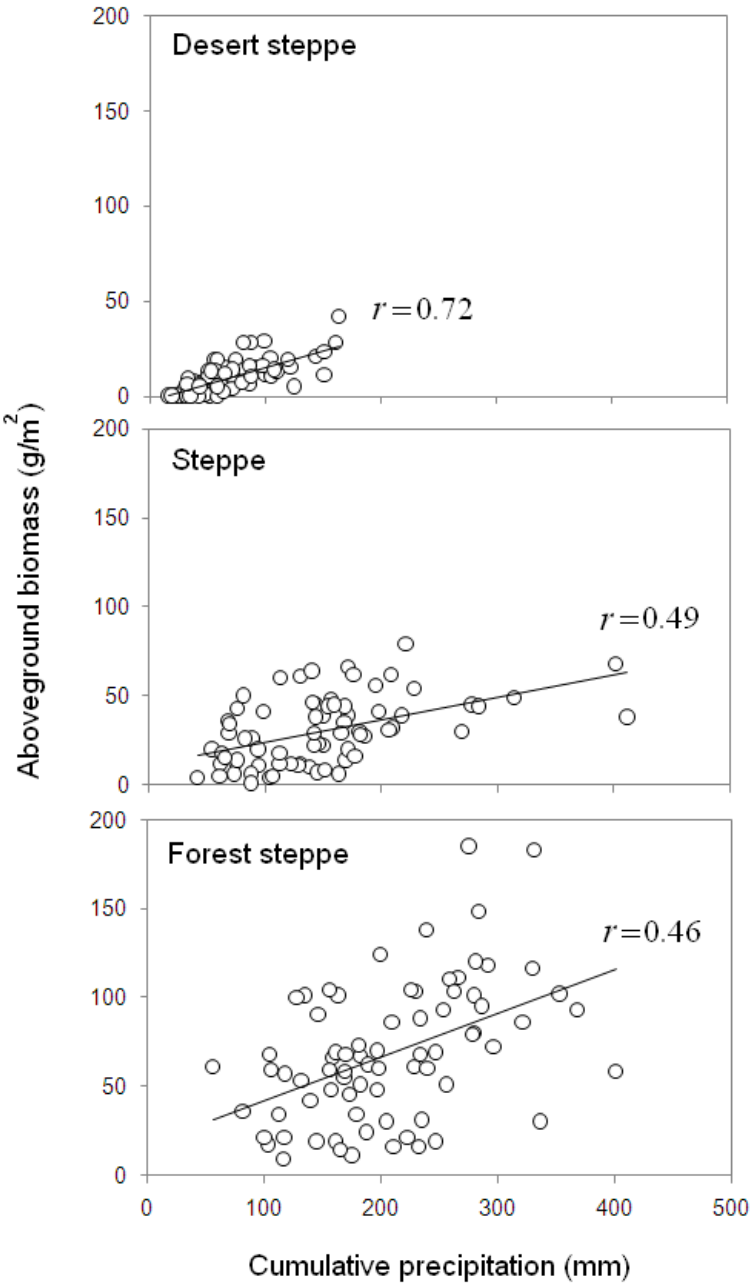


**Figure 2.2** Relationships between aboveground biomass (on 14 August) and cumulative precipitation (1 May–13 August) for five stations in each vegetation zone during 1986–2005.

**Table 2.3** Correlation of AGB and number of days with different precipitation amount (≤5 mm, 5.1–10 mm, and ≥10.1 mm) for each sites and for five sites in each vegetation zone during 1986–2005.

| Natural zone | Station name | ≤5 | 5.1-10 | ≥10.1 |
|---|---|---|---|---|
| Desert steppe | Gurvantes | 0.41 * | 0.45 * | 0.62 ** |
| | Mandalgovi | 0.54 * | 0.18 ns | 0.57 * |
| | Nogoonnuur | 0.40 ns | 0.03 ns | 0.59 * |
| | Tsogt-Ovoo | 0.37 ns | 0.29 ns | 0.54 * |
| | Zereg | 0.22 ns | 0.42 * | 0.52 * |
| | **Over five stations** | **0.57** *** | **0.40** *** | **0.60** *** |
| Steppe | Bayandelger | 0.19 ns | 0.52 ns | 0.61 ** |
| | Choibalsan | 0.16 ns | -0.17 ns | 0.58 * |
| | Khujirt | -0.27 ns | 0.61 ** | 0.46 * |
| | Ulaangom | -0.04 ns | 0.55 ns | 0.50 ns |
| | Underhaan | -0.19 ns | 0.16 ns | 0.68 ** |
| | **Over five stations** | **-0.04** ns | **0.30** * | **0.53** *** |
| Forest steppe | Bulgan | -0.37 ns | 0.22 ns | 0.56 * |
| | Dashbalbar | 0.17 ns | 0.51 * | 0.41 ns |
| | Erdenemandal | 0.18 ns | 0.50 * | 0.26 ns |
| | Kharhorin | 0.58 ns | 0.52 ns | 0.01 ns |
| | Tarialan | 0.33 ns | 0.35 ns | 0.60 ** |
| | **Over five stations** | **0.05** ns | **0.29** * | **0.41** *** |

* Correlation is significant at the 0.05 level, ** Correlation is significant at the 0.01 level, *** Correlation is significant at the 0.001 level, ns Correlation is not significant.

### 2.3.3 Grazing effect on aboveground biomass and plant height

The effects of grazing on AGB and plant height at Bayan Unjuul were examined based on detailed measurements from no-grazing and grazing plots. April to July precipitation was the highest in 2005 (65.3 mm, the wettest of the three years) and low in 2006 and 2007 (55.2 mm and 53.7 mm, respectively). In 2005, AGB and height were significantly larger in no-grazing plots than in grazing plots (Table 2.4). In 2006, AGB in no-grazing plots was significantly larger than in grazing plots, whereas height was not significantly different. However, in 2007 (a dry year), none of the values were

significantly different between the two types of plots. This suggests that, in 2007, there was less or no consumption of biomass by livestock due to low pasture availability in the Bayan Unjuul (steppe region); hence, herders moved with their animals into regions containing more pasture. It therefore indicates that grazing effects are controlled by pasture availability to livestock. This observation also suggests that species composition may be responsible for determining AGB. In 2007, unpalatable species such as *Salsola collina*, *Artemisia adamsii*, and *Chenopodium* spp. became more abundant in the grazing plots (accounting for 94% of the total AGB) compared with the no-grazing plots (49%). These species have high above-ground productivity and low below-ground productivity. It is therefore likely that species composition plays an important role in determining above- and below-ground biomass. However, further, more comprehensive, studies are needed to test this hypothesis.

**Table 2.4** Aboveground biomass (AGB) and plant height (Height) in no grazing (NG) and grazing (G) plots at Bayan Unjuul in July of 2005–2007. Different letters (a, b) refers significant difference ($p < 0.05$) between AGB, and Height of no grazing and grazing plots for each year.

| Date | AGB (g C/m$^2$) | | Height (cm) * | |
|---|---|---|---|---|
| | NG | G | NG | G |
| 21 July 2005 | 25.5$^a$ | 9.8$^b$ | 22$^a$ | 7$^b$ |
| 22 July 2006 | 15.0$^a$ | 6.1$^b$ | 14$^a$ | 10$^a$ |
| 28 July 2007 | 7.3$^a$ | 8.2$^a$ | 10$^a$ | 5$^a$ |

* Height refers to the average of the heights of the tallest individuals of every species for no grazing and grazing plots.

## 2.4 Conclusions

Precipitation and grazing are therefore important factors in determining pasture productivity. In general, the results of this study are consistent with those of previous

investigations, such as Fernandez-Gimenez and Allen-Diaz (1999) on biomass, Kondoh and Kaihotsu (2003) and Suzuki *et al*. (2007) on NDVI, Miyazaki *et al*. (2004) on Leaf area index (LAI), and Chen *et al*. (2007) on grazing. All of these studies reported that inter-annual changes in plant growth are related to changes in precipitation and grazing.

# CHAPTER 3

## Relationship between photosynthetically active radiation and global solar radiation

## 3.1 Introduction

The accurate determination of PAR is important in many applications, such as estimating NPP and carbon cycle modeling (Pinker and Laszlo, 1992; Frouin and Pinker, 1995). In the absence of a worldwide routine network for measuring PAR, this parameter is often calculated indirectly based on its relationship with SR. Forty-four percent of incoming solar energy is believed to occur between 400 nm and 700 nm at low altitudes (Moon, 1940), and photosynthetically useful radiation is thought to account for half of all SR (Monteith,1973). As determined by McCree (1966), the average PAR/SR is 0.48, varying from 0.47 to 0.59, with the highest values occurring during cloud-covered sky. Other studies have found that PAR/SR is not constant, but varies according to location (Tsubo and Walker, 2005), season (Udo and Aro, 1999; Finch *et al*., 2004), sky conditions (Rao, 1984; Papaioannou *et al*., 1993), altitude (Wang *et al*., 2007), and irradiance intensity (Britton and Dodd, 1976). This spread of PAR/SR reported in the literature suggests that the relationship between PAR and SR needs to be calibrated according to local climatic conditions. As such, it is important to analyze the characteristics of PAR with directly measured data and to develop an appropriate model for estimating PAR from

SR. The aim of this chapter is therefore to determine PAR/SR and to investigate its dependence on sky condition and atmospheric water vapor.

## 3.2 Data collection and calculation

Global PAR (0.4–0.7 μm in wavelength) and global SR (0.3–3.0 μm in wavelength) were recorded at the Bayan Unjuul study site (47°02′37.2″N, 105°57′04.9″E, 1200 masl) using a quantum sensor (LI190SZ, LI-COR, USA), and a pyranometer mounted in CNR-1 (company) Net Radiometer. The study site has its own significant features; such as semi-arid climate (UNEP 1992), high altitude, low temperature, good air transparency, and strong solar radiation. Summer season has a long daytime and sunshine, while winter has a short day but mostly clear days due to high pressure system.

PAR was expressed by quantum flux (μmol/$m^2$/s) whereas SR was expressed energy flux (W/$m^2$). Therefore, for comparison PAR photon flux was converted into its energy flux using conversion factor of 0.2195 (Ross and Sulev, 2000).

Daily extraterrestrial SR on a horizontal surface was estimated from the solar constant, the solar declination and the day of the year as expressed by following equation (Allen *et al*., 1998):

$$R_a = \frac{24(60)}{\pi} G_{SC} d_R [\omega_S \sin(\varphi)\sin(\delta) + \cos(\varphi)\cos(\delta)\sin(\omega_S)] \quad (3.1)$$

where $R_a$ is extraterrestrial radiation (MJ/$m^2$/day), $G_{SC}$ is solar constant (0.0820 MJ/$m^2$/min), $\varphi$ is latitude (radians), $d_R$ is inverse relative distance Earth-Sun (equation 3), $\omega_S$ is sunset hour angle (radians), $\delta$ is solar declination (radians). The conversion from decimal degrees to radians is given by:

$$[Radians] = \frac{\pi}{180}[DecimalDegrees] \quad (3.2)$$

The inverse relative distance Earth-Sun, $d_R$, and the solar declination, $\delta$, are given by:

$$d_R = 1 + 0.033\cos(\frac{2\pi}{365}J) \quad (3.3)$$

$$\delta = 0.409\sin(\frac{2\pi}{365}J - 1.39) \quad (3.4)$$

where $J$ is the number of the day in the year between 1 (1 January) and 365 or 366 (31 December). The sunset hour angle, $\omega_S$, is given by:

$$\omega_S = \frac{\pi}{2} - \arctan\left[\frac{\tan(\varphi)\tan(\delta)}{X^{0.5}}\right] \quad (3.5)$$

where

$$X = 1 - [\tan(\varphi)]^2[\tan(\delta)]^2 \quad (3.6)$$

## 3.3 Results and discussion

Figure 3.1 shows monthly extra-terrestrial and global SR and global PAR at Bayan Unjuul, from July 2004 to June 2005. The radiation parameters show similar seasonal variations, with a peak in July (1250 MJ/m$^2$/month of extra-terrestrial SR, 734 MJ/m$^2$/month of global SR, and 336 MJ/m$^2$/month of PAR) and a low in December (293 MJ/m$^2$/month, 177 MJ/m$^2$/month, and 74 MJ/m$^2$/month, respectively). In comparison, a study of monthly global PAR (47°N) by Tugjsuren and Takamura (2001) found that

values were slightly higher in Bayan Unjuul than at Ugtaal, Mongolia (48°N), where it varied from 69 to 307 MJ/m$^2$/month.

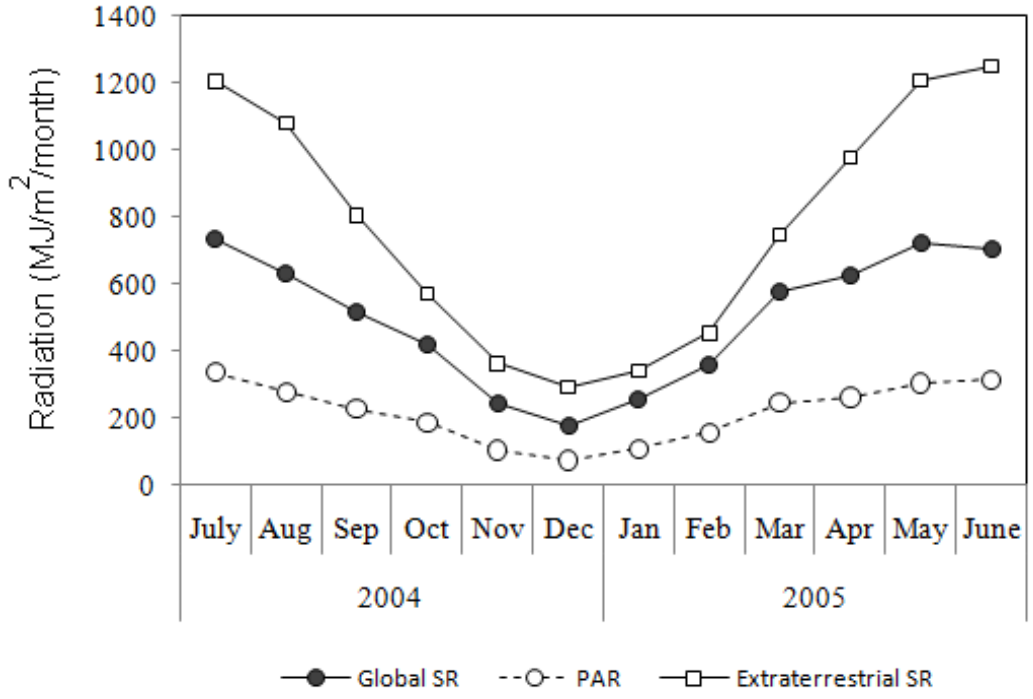


**Figure 3.1** The trend in monthly extraterrestrial and global SR and global PAR at Bayan Unjuul, Mongolia from July 2004 to June 2005.

The monthly mean diurnal variations of PAR/SR showed that PAR/SR mainly approached its higher and lower values during sunrise and sunset hours. The ratios showed slight diurnal variation during June–September (Figure 3.2) and they reached their lowest value around noon. These results are similar to those of previous studies (Udo and Aro, 1999; Wang *et al.*, 2007).

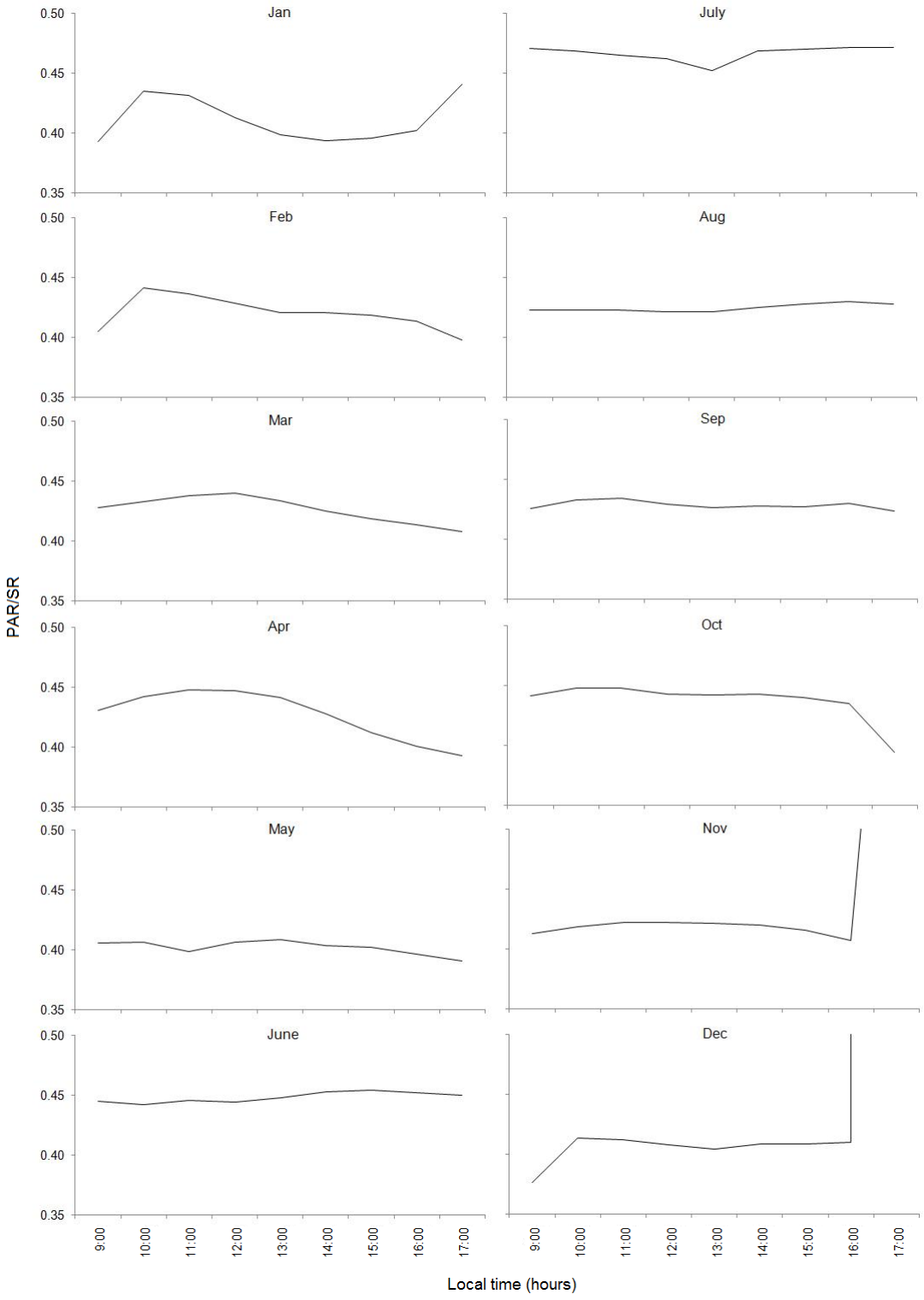


**Figure 3.2** Monthly mean diurnal variation of the PAR/SR.

Daily PAR/SR (averaged over each month) ranged from 0.42 in April and December to 0.459 in July, with the growing season average of 0.438±0.013 and annual mean value of 0.434±0.013 (Table 3.1). Due to the region's dry climatic condition, the annual mean PAR/SR was lower than those most previous studies, typically falling between 0.45 and 0.50. However it was close to the value of 0.43 for Athens, Greece; 0.437 for Sweden; and 0.44 for Fresno, USA and Aas, Norway. The annual range of PAR/SR was similar to that in Sweden (Rodskjer, 1983), Norway (Hansen, 1984), Greece (Papaioannou *et al*., 1996), Nigeria (Udo and Aro, 1999) and Tibet (Zhang *et al*., 2000).

**Table 3.1** Monthly and seasonal mean of the PAR/SR and water vapor pressure.

| Year | Month | PAR/SR | Water vapor pressure (hPa) |
|---|---|---|---|
| 2004 | July | 0.459 ± 0.016 | 11.86 |
| | Aug | 0.439 ± 0.016 | 9.61 |
| | Sep | 0.438 ± 0.012 | 6.07 |
| | Oct | 0.449 ± 0.012 | 3.28 |
| | Nov | 0.429 ± 0.014 | 1.92 |
| 2005 | Dec | 0.420 ± 0.015 | 1.32 |
| | Jan | 0.425 ± 0.017 | 0.95 |
| | Feb | 0.437 ± 0.015 | 0.65 |
| | Mar | 0.427 ± 0.016 | 2.18 |
| | Apr | 0.420 ± 0.016 | 3.31 |
| | May | 0.421 ± 0.010 | 4.68 |
| | June | 0.448 ± 0.020 | 8.32 |
| | Apr–Sep | 0.438 ± 0.013 | 8.11 ± 2.54 |
| | Annual | 0.434 ± 0.013 | 4.51 ± 3.69 |

Atmospheric parameters such as water vapor and cloud cover have the greatest influence on the PAR fraction (Alados *et al*., 1996). In the present study, the clearness index (the ratio of global SR to extra-terrestrial SR) was used to characterize sky

conditions, revealing a significant and negative correlation with PAR/SR ($r$ = -0.36, $p$ < 0.05) (Figure 3.3).

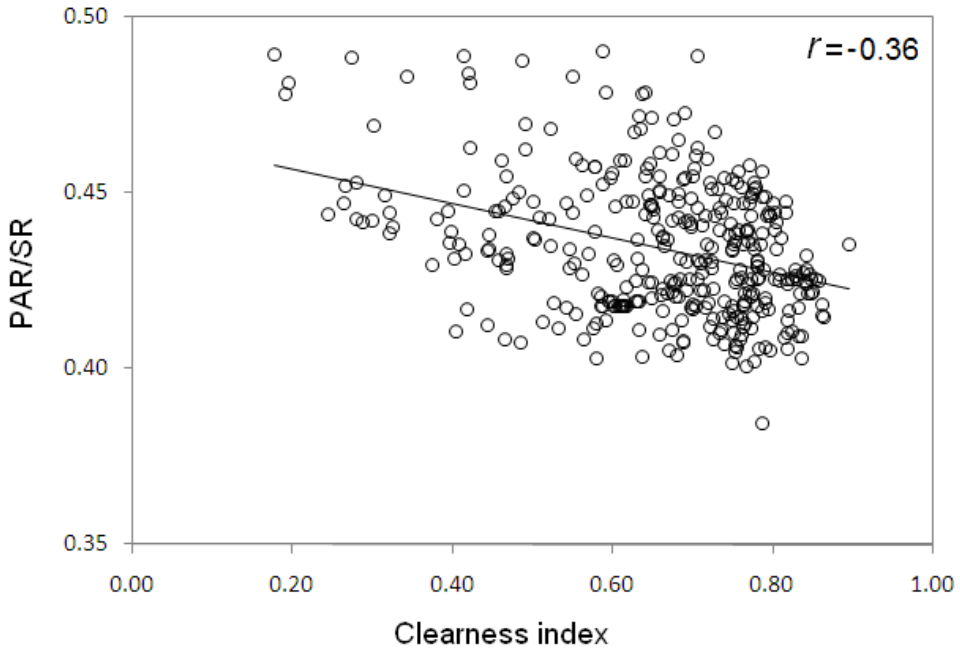


**Figure 3.3** Relationship between the PAR/SR and the clearness index.

Furthermore, to investigate the effect of sky condition on PAR/SR, the clearness index was divided into three equal classes ($0.18 < K_T < 0.33$ for cloudy days; $0.34 < K_T < 0.66$ for partly cloudy days; and $0.67 < K_T < 0.90$ for clear or nearly clear days). Sixteen days were cloudy, 139 were partly cloudy, and 210 days were clear or nearly clear. PAR/SR increased from 0.432 on clear days to 0.440 on partly cloudy days and 0.465 on cloudy days (Figure 3.4). An increase in PAR/SR under cloudy conditions has also been reported in previous studies by Hu *et al*. (2007), Papaioannou *et al*. (1993), and Tsubo and Walker (2005). However, the effect of the clearness index on PAR/SR was negligible on a daily basis for Fresno, California, USA (Howell *et al*., 1983). A significant correlation was found between PAR/SR and water vapor pressure ($r$ = 0.48, $p$ < 0.05) (Figure 3.5).

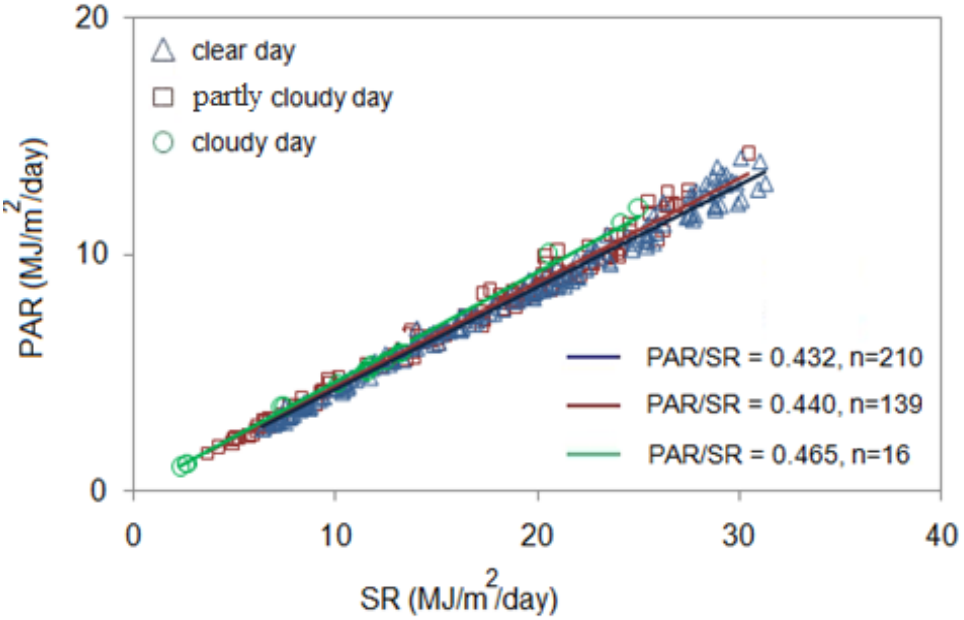


**Figure 3.4** Relationship between daily PAR and SR under different sky conditions.

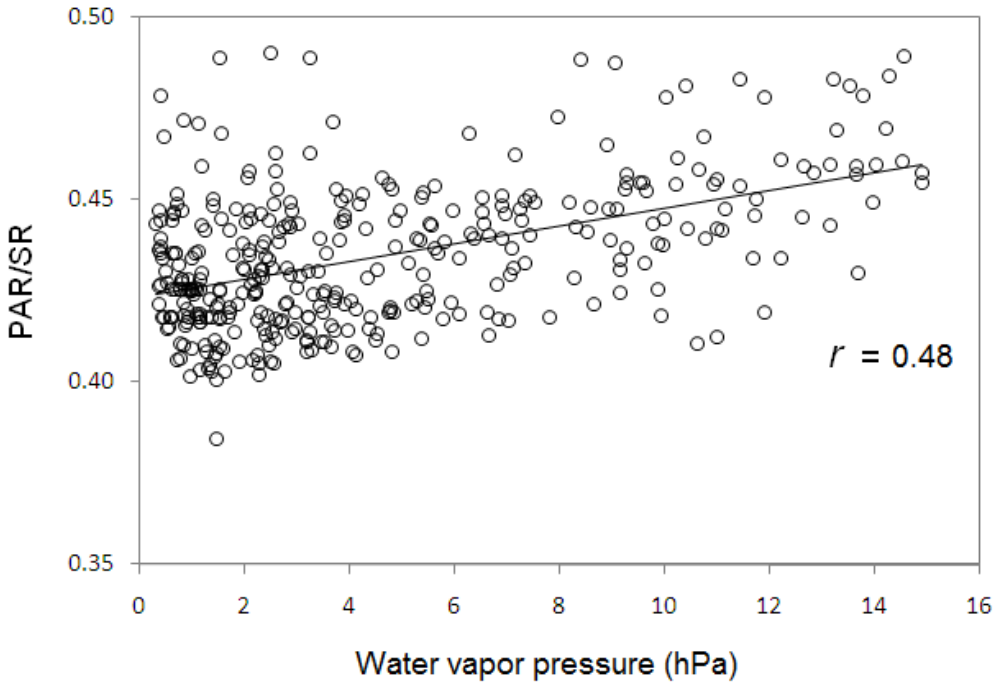


**Figure 3.5** Relationship between the PAR/SR and the water vapor pressure.

As shown Table 3.1, the lower values of PAR/SR (0.420–0.437) mainly appeared during November–May under dry conditions, whereas the higher PAR/SR (0.438–0.459) was observed from June to October under cloudy and humid conditions. Similar variations in PAR/SR have been reported for Beijing (Hu *et al*., 2007), where lower PAR/SR was observed during the dry season and higher PAR/SR occurred in the wet season. Thus, in Beijing, PAR/SR is controlled mainly by water vapor in the atmosphere (represented by relative humidity).

At the study site, it is likely that the increases in PAR/SR were found under cloudy and humid conditions because absorption of SR in the near infrared radiation (NIR) portion of the solar spectrum is enhanced, whereas water vapor is almost transparent to PAR wavelengths.

# CHAPTER 4

## Effects of water and temperature stresses on radiation use efficiency[1]

## 4.1 Introduction

Many models have been developed to simulate the productivity of different ecosystems; among these models, those that focus on production efficiency are the simplest and most commonly used methods for analyzing and modeling plant growth over space using ground and satellite remote-sensing-based data. In the beginning, (Monteith, 1972, 1977) explored a simple PEM of primary production for crops. This has provided the basis for many models, such as Carnegie Ames Stanford Approach (CASA) (Potter *et al*., 1993) and GLObal Production Efficiency Model (GLO-PEM) (Prince and Goward, 1995), which are using remote-sensing data to estimate ecosystem productivity. Such models rely on inputs of incident PAR, *fIPAR*, and RUE. Fraction of IPAR is often

[1] This chapter is edited version of
Tserenpurev Bat-Oyun, Masato Shinoda, Mitsuru Tsubo (2011), Effects of water and temperature stresses on radiation use efficiency in a semi-arid grassland, *Journal of Plant Interactions*,
DOI: 10.1080/17429145.2011.564736

calculated as a linear function of the remote-sensing-based NDVI (Asrar *et al*., 1984; Goward and Huemmrich, 1992; Prince and Goward, 1995). RUE, another major component of the PEM, can be used to evaluate the efficiency of photosynthesis and plant production limitations under different seasonal and environmental conditions (Runyon *et al*. 1993; Sinclair and Muchow, 1999). The initial studies indicated that RUE might be relatively constant across a range of plant types (Monteith, 1972), but broader studies have revealed more than fivefold variation depending on the biome type (Gower *et al*., 1999), growth stage (Jeuffroy and Ney, 1997), and levels of various environmental stresses (Akmal and Janssens, 2004). RUE varies over a relatively narrow range for crop systems, but over a wider range for natural ecosystems due to the larger variation in the levels of environmental stresses (Russell *et al*., 1989).

In Mongolia, grasslands cover approximately 80% of the country (Batima and Dagvadorj, 2000) under arid and semi-arid climate (UNEP, 1992). The production of grassland is regulated by many factors, such as precipitation, temperature, solar radiation, soil nutrient availability, and grassland utilization and management. Among these water stress is the most critical limiting factor determining the efficiency of photosynthetic radiation utilization and the vegetation productivity in drylands due to the low precipitation and high evapotranspiration (Noy-Meir, 1973; Li *et al*., 2008; Nakano *et al*., 2008). Water deficiency in plants restricts their potential carbon assimilation by affecting photosynthetic processes through decreased stomatal conductance, which not only decreases photosynthesis but also slows respiration and water loss per unit area (Day *et al*., 1981). Nakano *et al*. (2008) demonstrated that a reduction in the gross primary production per unit of AGB was caused by a combination of high atmospheric vapor pressure deficit (VPD) and low soil moisture condition, while (Shinoda *et al*., 2010b) reported that drought drastically reduced aboveground phytomass of grasslands. When soil moisture

availability exceeded VPD, grasses used PAR more efficiently in a Mongolian grassland (Li *et al*., 2008), indicating that drought induces a decline in RUE for grassland ecosystems.

Temperature is another environmental factor which affects on RUE. Excessively high and low temperatures can both result in poor plant growth by slowing down photosynthetic processes (Farquhar *et al*., 1980). Low temperatures reduced RUE for different types of crops (Andrade *et al*., 1992; Bell *et al*., 1992). For example, (Andrade *et al*., 1992) showed that the temperature from 15 to 18°C during the vegetative period caused low RUE in maize. Also, high temperature (increased respiration sometimes above the rate of photosynthesis) had negative effects on crops (Pastenes and Horton, 1996; Monneveux *et al*., 2003). In a previous study, decreased precipitation as combined with high temperature showed a considerable negative effect on pasture production in southern Mongolia (Munkhtsetseg *et al*., 2007).

A few studies have been conducted on RUE for semi-arid grasslands, especially on direct comparisons of RUE under well-watered and water stressed conditions. The failure to adequately address variation in RUE often led to large errors in the estimates of net primary production (Nouvellon *et al*., 2000). Therefore, comprehensively determining RUE in natural grasslands in a dry region is a research priority. As compared with temperature stress, water stress is a strong down-regulator of NPP in the Mongolian grasslands (Bat-Oyun *et al*., 2010). Thus, we expected that water stress would be the primary factor influencing RUE. Given this background, the objectives of this chapter were to investigate the effects of water and temperature stresses on vegetation growth and radiation interception in grassland; examine the relationship between *fIPAR* and NDVI; and quantify RUE.

# 4.2 Materials and methods

## 4.2.1 Site description

An observation site (30 m by 30 m with a fence to protect against biotic factors such as livestock grazing and human effects) was established at Bayan Unjuul (47°02′37.2″N, 105°57′04.9″E, 1200 masl) in the steppe zone of Mongolia (Figure 4.1a, b) to carry out field experiments in 2009 and 2010. The region's climate is semi-arid according to the aridity index ranging between 0.2 and 0.5 (UNEP 1992) and its steppe vegetation (Yunatov, 1976).

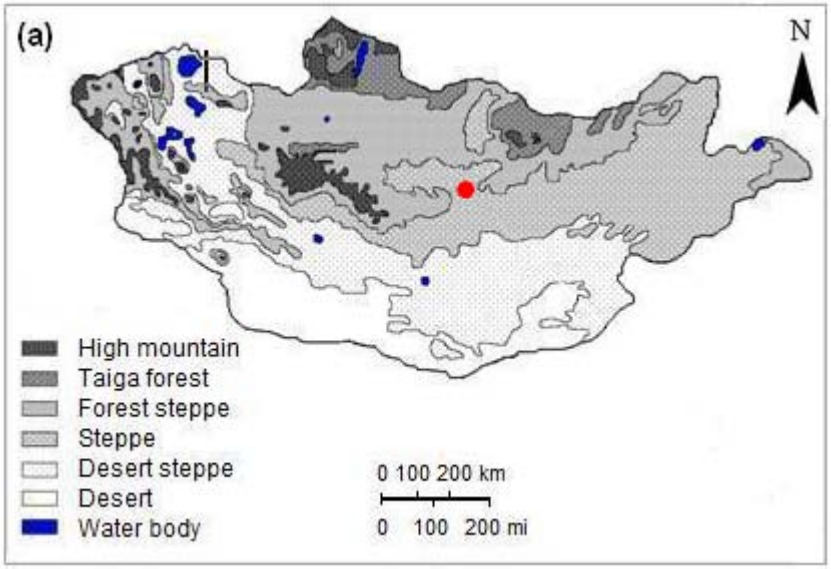


**(b)**

**Figure 4.1** (a) Vegetation map of Mongolia. Location of the study site (47°02′37.2″N, 105°57′04.9″E, 1200 masl) is shown as red dot. (b) The study site at Bayan Unjuul in August 2009.

The site is characterized by low annual precipitation, with high inter- and intra-seasonal variability, frequent droughts, and sandy, nutrient-poor soils (Shinoda *et al*., 2010a), hence low water-holding capacity of the soil, and the sparse vegetation cover associated with low leaf area. Generally, the growing season for the Mongolian grasslands is very short (May–August) and it is limited by low temperature and precipitation (Shinoda *et al*., 2007). The long-term (1995–2008) average air temperature and precipitation were 16.9°C and 119 mm, respectively during the growing season. The vegetation of Bayan Unjuul is codominated by perennial grasses such as *Stipa krylovii*, *Agropyron cristatum* and *Cleistogenes squarrosa*, forbs such as *Artemisia adamsii*, *Salsola collina* and *Chenopodium aristatum*, and a small shrub, *Caragana stenophylla* (pictures of plant species shown in Appendix C on pages 80−82).

### 4.2.2 Experimental design and water-stress treatments

Irrigation experiments were conducted in the enclosure during the periods from 1 May to 10 August 2009 and from 1 May to 18 August 2010. Wide borders were used to minimize any edge effects: a 2.25-m-wide border from the northern and southern sides of the fence, a 3.5-m-wide border on the eastern and western sides, and a 3-m-wide gap to prevent interference between adjacent irrigation treatments. Plant growth and species composition were uniform inside the enclosure when the fence was established. Vegetation in the study site consisted of many species mentioned above; however forbs such as *S. collina, A. adamsii* and *C. aristatum* were codominated in the study years. The experimental layout was a randomized complete block design, consisting of three water treatments with four blocks (replications); each block contained eight sample plots (Figure 4.2). In 2010 the experimental plots were shifted to avoid the effects of biomass sampling and irrigation treatment in the previous season.

The field experiments were carried out in the natural vegetation, so there was no information on the plant water requirement for maximizing the productivity. To simulate plant response to various soil water environments, experimental treatments with two different amounts of irrigation water were set in each year. The irrigation amounts were determined from the depth of precipitation. The three water treatments were rainfed (control-only precipitation), low-irrigation (80 and 30% more water than the controls in 2009 and 2010, respectively) and high-irrigation (160 and 60% more water than the controls, respectively). Precipitation during the experiment periods was 124 mm in 2009 and 110 mm in 2010, so 99 and 33 mm of irrigation water were added to the low-irrigation plots, respectively, and 198 and 66 mm to the high-irrigation plots.

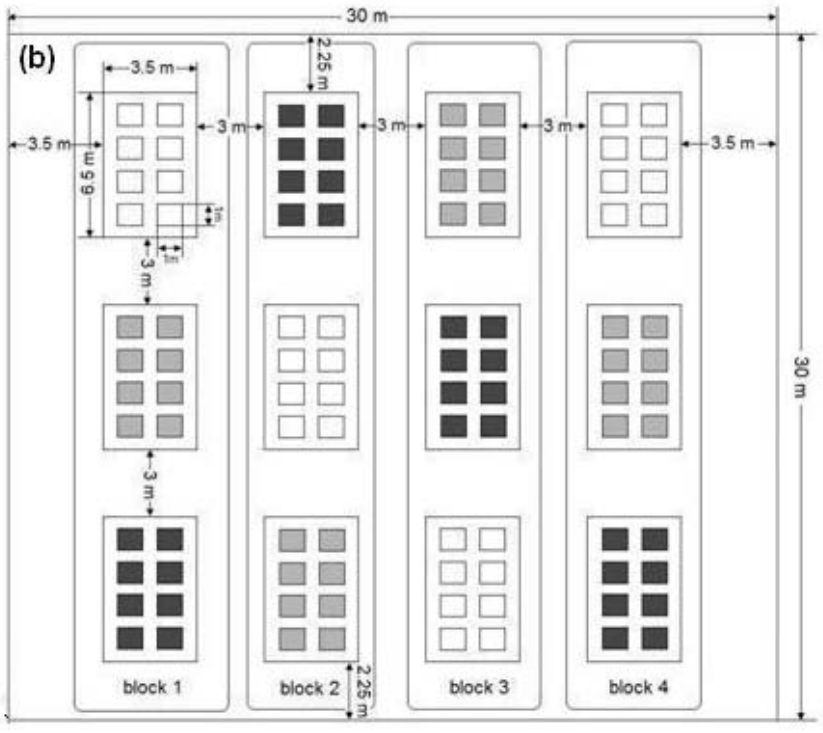


**Figure 4.2** Illustration of the experimental design. The plots with light gray and dark gray shades correspond to low and high levels of irrigation, respectively. The unshaded areas correspond to control (non-irrigation) plots.

The relationship between AGB and precipitation event size demonstrated that AGB did not alter at low precipitation levels ($\leq 5$ mm), whereas large precipitation event ($\geq 5$ mm) tended to make significant contribution on its growth for the steppe region (Chapter 2). Nakano *et al*., (2008) and Shinoda *et al*., (2010b) reported that low precipitation (<5 mm) did not contribute to SWC at 10 cm depth at the study site. Considering these point, at least 5 and 10 mm/day irrigation water was applied for the low and high-irrigation plots, respectively. During the study periods, irrigation was applied 7 and 6 times in 2009 and 2010, respectively, at intervals of 5 to 17 days.

### 4.2.3 Data collection and calculations

Air temperature and precipitation data were obtained from a meteorological station (450 m southeast of the observation site) operated by the Mongolian Institute of Meteorology and Hydrology. Before and after irrigation, volumetric SWC in the 0–16 cm soil layer was measured at four plots in each treatment using a time-domain reflectometer (TRIME-EZ, IMKO, Germany).

In order to determine IPAR, PAR (0.4 to 0.7 μm) was measured above and beneath the plant canopy with AccuPAR LP-80 ceptometer (Decagon Devices Inc., Pullman, Washington, USA). A single quantum sensor was set to the top of the canopy, and the line quantum sensor (composing 80 independent sensors spaced 1 cm apart) was placed below the canopy (Figure 4.3). Before each radiation measurement, dead and brown plant material was removed from the experimental plots. All radiation measurements were taken at hourly intervals between 10:00 and 15:00 local standard time on clear days.

The measurements were conducted before biomass sampling eight times during the experimental period. During the study period, AGB sampling was conducted eight times, at intervals of 7 to 18 days. The aboveground part of plants was clipped in 1 m by 1 m

quadrats. No one area was sampled twice. Belowground biomass (BGB) was measured immediately after the AGB sampling by excavating all roots in the top 0–10 and 10–20 cm of the soil layers. The area of BGB sampling was 50 cm by 50 cm within the 1 m by 1 m quadrat for the AGB. The sampled materials were sieved through a 0.3 cm-by-0.3 cm mesh, and the soil was washed away. The BGB was collected 5 and 4 times during the growing seasons of 2009 and 2010, respectively. All collected plant materials were oven-dried at 80°C for 3 days and were then weighed to determine the dry matter.

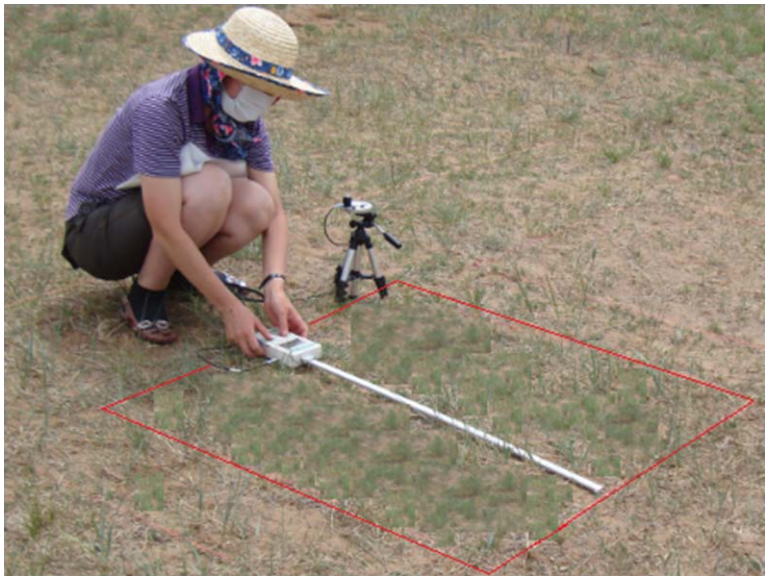

**Figure 4.3** Measuring the above and below canopy PAR with AccuPAR LP-80 ceptometer in the field.

### 4.2.4 Soil moisture

Nandintsetseg and Shinoda (2010) modified an existing one-layer water balance model developed for low-latitude arid regions (Yamaguchi and Shinoda, 2002) to represent the extratropical characteristics of winter soil freezing and spring snowmelt in Mongolia. This model requires daily precipitation and air temperature data with a limited number of measured soil parameters to calculate plant available soil water content

(PASWC). SWC is defined as PASWC plus SWC at wilting point (mm) [hereinafter referred to as estimated SWC]. In the present study, this model was applied to the study site.

According to the measurement of BGB in 0–10 and 10–20 cm soil layers at the study site in 2009 and 2010, more than 80% of BGB was distributed within the top 10 cm of soil layer. Therefore, assuming that the top 20 cm of the soil is a major rooting zone, SWC of the rooting zone was estimated. The water balance model was validated with SWC data measured at the 10 cm depth at NG site adjacent to our experimental plots.

### 4.2.5 Radiation interception

The *fIPAR* was calculated, as follows:

$$fIPAR = (I_0 - I_t) / I_0 \quad (4.1)$$

where Io and It are the PAR measured above and below the canopy, respectively. Daily IPAR was calculated by multiplying daily incident PAR by daily *fIPAR*. Daily *fIPAR* was estimated by linear interpolation between two consecutive measurements of *fIPAR*. Finally, the daily IPAR values were summed to obtain a cumulative IPAR for each part of the experimental period. Incident PAR was recorded at the NG site with a quantum sensor (LI190SZ, LI-COR, USA) at the 1.5 m height.

### 4.2.6 Radiation use efficiency

Radiation use efficiency is the efficiency of plant to change the solar energy into organic dry matter (carbon) through photosynthesis. RUE (g/MJ IPAR) was estimated as

the slope of the linear regression between the AGB and the cumulative IPAR, which is most appropriate method as reviewed by Sinclair and Muchow (1999). Then, maximum RUE ( $\varepsilon_{MAX}$ ) was determined using the following equation:

$$\varepsilon_{STRESS} = \varepsilon_{MAX} \cdot f_{WS} \cdot f_{TS} \tag{4.2}$$

where $\varepsilon_{STRESS}$ is estimated RUE, and $f_{WS}$ and $f_{TS}$ are water and temperature stress factors, respectively (ranging between 0 and 1; lower values indicate a higher degree of stress).

In order to quantify $f_{WS}$, the following equation was used (Allen *et al*., 1998):

$$f_{WS} = \begin{cases} (\theta_i - \theta_{WP})/(\theta_T - \theta_{WP}) & \theta_i < \theta_T \\ 1, & \theta_i \geq \theta_T \end{cases} \tag{4.3}$$

$$\theta_T = (1-p) \cdot \theta_{FC} + p \cdot \theta_{WP}$$

where $\theta_i$ is SWC for a period i, $\theta_{WP}$ and $\theta_{FC}$ are SWC at wilting point and field capacity, respectively [in this study, 4.85 and 20.48%, respectively, calculated with the method of (Saxton *et al*., 1986)], $\theta_T$ is threshold SWC to initiate water stress, and p is average fraction of total available soil water that can be depleted from the root zone before water stress (reduction in evapotranspiration) occurs (in this study, p = 0.3 for shallow rooted grasses, i.e. $\theta_T$ = 15.79%).

RUE strongly depends on air temperature, as photosynthesis is affected by temperature. Jones (1992) described an empirical equation to estimate temperature effect on net photosynthesis, and this equation was used to quantify the effect of temperature stress on RUE:

$$f_{TS} = \frac{2(T_{obs} - T_{base})^2 (T_{opt} - T_{base})^2 - (T_{obs} - T_{base})^4}{(T_{opt} - T_{base})^4} \quad (4.4)$$

where $T_{obs}$ is average temperature, $T_{base}$ is base temperature, and $T_{opt}$ is optimum temperature, when the coefficient reaches a maximum of 1. The plant growth starts above 5°C at the steppe vegetation zone of Mongolia, while the ratio of gross primary production to AGB reached its maximum around 27°C (Nakano *et al*., 2008), which was consistent with the values for C3 and desert plants (Larcher, 2003). An optimum temperature for C3 plants also ranges from 20°C to 25°C (Devlin and Barker, 1971). In this study $T_{base}$ and $T_{opt}$ were therefore assumed to be 5°C and 25°C, respectively.

### 4.2.7 NDVI

Reflectance of spectral irradiance ($W/m^2/nm$) of the canopy was measured using a portable spectroradiometer (MS-720, EKO Instruments Co. Ltd., Phoenix, Arizona, USA). The sampling wavelength range is 350–1050 nm and its spectral resolution is 1 nm. The spectroradiometer held in a nadir orientation above the vegetation surface. The mean reflectance was calculated as the average of four replicates. NDVI was derived from these measurements using the following equation:

$$NDVI = (\rho_{NIR} - \rho_{RED})/(\rho_{NIR} + \rho_{RED}) \quad (4.5)$$

where $\rho_{NIR}$ is the reflectance for near-infrared radiation, and $\rho_{RED}$ is the reflectance for red radiation. In the Advanced Very High Resolution Radiometer (NOAA/AVHRR) NDVI products, $\rho_{NIR}$ and $\rho_{RED}$ correspond to band 2 (725–1000 nm) and band 1 (580–680 nm),

respectively. These ranges were used in our observed spectral irradiance data to compute NDVI values for each treatment.

### 4.2.8 Statistical analysis

Statistically significant differences in biomass and radiation interception between the different treatments were determined by the Tukey's method at the 5% significance level using SPSS® and JMP IN® statistical software. For the comparison of the estimated parameters with the measured parameters, the correlation-based statistic (coefficient of determination, $r^2$) was used with the deviation-based statistic (root mean square error, RMSE) (Willmott, 1982).

## 4.3 Results

### 4.3.1 Meteorological and soil water conditions

Figure 4.4a-f presents the seasonal changes in water (precipitation and irrigation) and measured and estimated SWC for the three water treatments in 2009 and 2010. During the first period (1 May–8 July) and second period (9 July–9 August) of the experiment in 2009, 43 and 81 mm of precipitation (35 and 65% of the total) were recorded, respectively. Thus, in conjunction with precipitation, additionally 34 and 65 mm (about 80% of precipitation) of irrigation water in the low-irrigation plots versus 68 and 130 mm (160%) in the high-irrigation plots were applied during the first and second periods of 2009, respectively (Table 4.1). During the first period (1 May–4 July) and second period (5 July–18 August) of the experiment in 2010, 22 and 88 mm of precipitation (20 and 80% of the total) were recorded. Additionally 15 and 18 mm of irrigation water in the low-irrigation plot versus 30 and 36 mm in the high-irrigation plot were applied during the first

and second periods of 2010, respectively (Table 4.1). Finally, low- and high-irrigation plots received 30 and 60% more water than control during the experiment period of 2010. Therefore, all treatments received high amount of water in 2009 than in 2010.

The water balance model represented well the detailed variations in the precipitation events and seasonal variations in the observed SWC measured at the NG site (Figure 4.4a, d). The estimated SWC was also similar with the measured SWC in the experimental plots (Figure 4.4) and the correlation coefficient between them was statistically significant ($r^2$ = 0.91, $p$ < 0.05) with the RMSE of 1.48% (Figure 4.5). Therefore, the model estimations were able to represent continuous seasonal changes of SWC for each treatment.

The PASWC estimated by the water balance model was low during the first period (3.4, 5.0 and 6.2% in 2009; 2.2, 2.8 and 3.3% in 2010 for the control, low-irrigation and high-irrigation plots, respectively), whereas the corresponding values were high during the second period (6.7, 10.4 and 11.6% in 2009; 5.6, 7.0 and 8.0% in 2010). SWC in the control plots, and low- and high-irrigation plots in 2010 mostly remained between $\theta_{WP}$ and $\theta_T$ (Figure 4.4a, d, e, f), whereas in the low- and high-irrigation plots in 2009 it frequently exceeded the $\theta_T$ and occasionally reached $\theta_{FC}$ after intense precipitation or irrigation (Figure 4.4b, c).

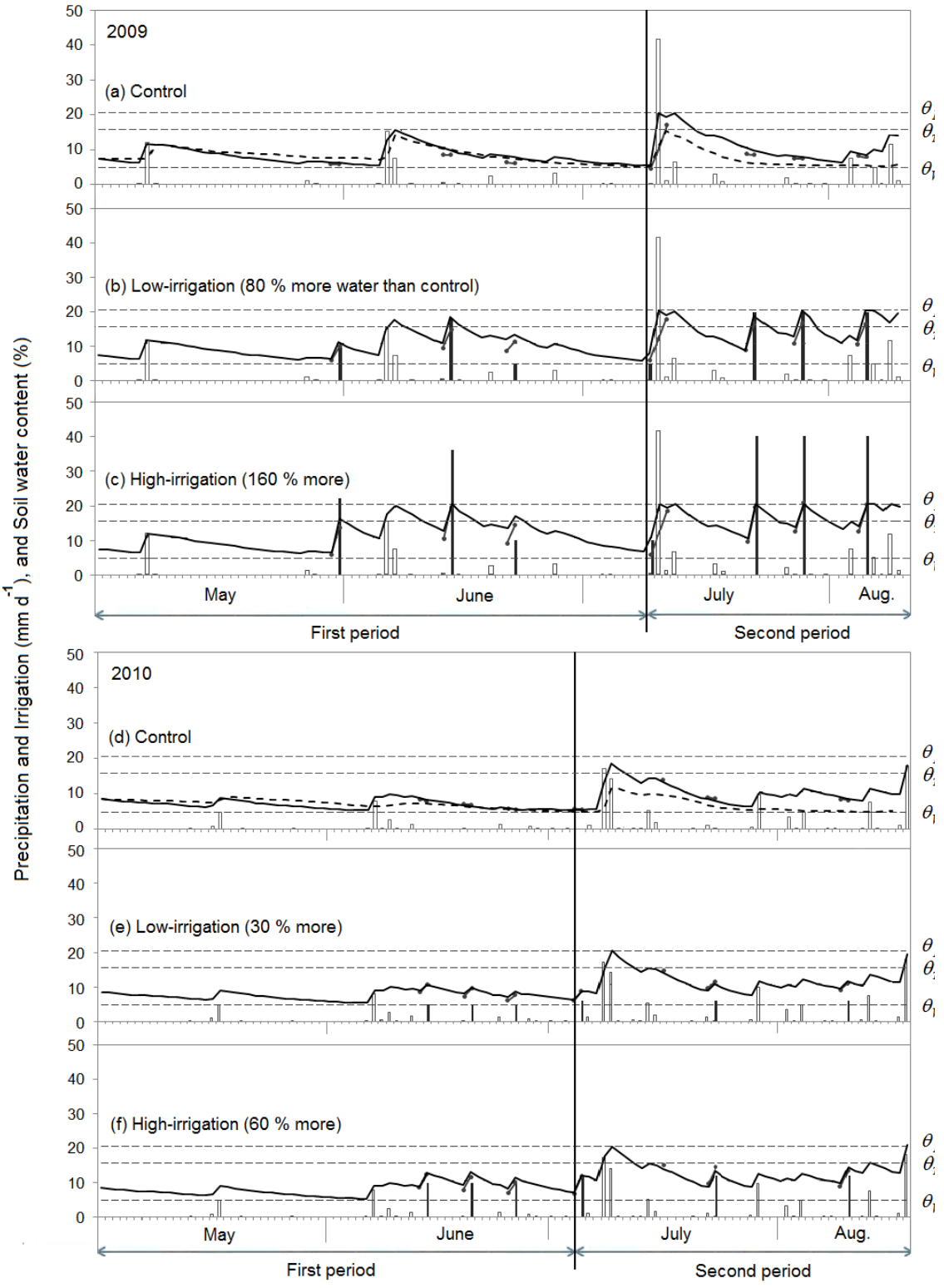


**Figure 4.4** Time series of (a, d) daily precipitation (white bars), SWC at the depth of 10 cm measured at the non-grazing site (dashed lines), measured SWC before and after irrigation in the soil layer of 0–16 cm depth at the study site (black cycles) and estimated SWC in the soil layer of

the 0–20 cm depth (solid lines) in the control plot; and time series of (b, c, e and f) daily precipitation, irrigation (black bars) and measured and estimated SWC in the low-irrigation and high-irrigation plots in 2009 and 2010. Horizontal dashed lines denote SWC at the field capacity ( $\theta_{FC}$ , 20.5%), permanent wilting point ( $\theta_{WP}$ , 4.9%), and threshold SWC ( $\theta_T$ , 15.8%), respectively. The periods from 1 May to 8 July 2009 and from 1 May to 4 July 2010 are the first periods, whereas the periods from 9 July to 9 August 2009 and from 5 July to 18 August 2010 are the second periods.

**Table 4.1** Water amount (precipitation (mm) for the control, precipitation plus irrigation (mm) for the low- and high-irrigation treatments), average air temperature (°C), water and temperature stress factors ( $f_{WS}$ , $f_{TS}$ ), estimated RUE ( $\varepsilon_a$ , g AGB/MJ IPAR) and estimated maximum RUE ( $\varepsilon_{MAX}$ , g AGB/MJ IPAR) during the first and second periods in 2009 and 2010.

| Year | Period | Treatments | Water amount | Temperature | $f_{WS}$ | $f_{TS}$ | $\varepsilon_a$ | $\varepsilon_{MAX}$ |
|---|---|---|---|---|---|---|---|---|
| 2009 | First | Control | 43 | 15.8±5.4 | 0.31 | 0.50 | 0.33 | 2.13 |
| | | Low-irrigation | 77 | | 0.41 | 0.50 | 0.45 | 2.20 |
| | | High-irrigation | 111 | | 0.54 | 0.50 | 0.57 | 2.11 |
| | Second | Control | 81 | 19.8±2.7 | 0.56 | 0.82 | 1.06 | 2.31 |
| | | Low-irrigation | 146 | | 0.86 | 0.82 | 1.74 | 2.47 |
| | | High-irrigation | 211 | | 0.94 | 0.82 | 2.05 | 2.66 |
| 2010 | First | Control | 22 | 16.4±6.6 | 0.20 | 0.50 | 0.23 | 2.30 |
| | | Low-irrigation | 37 | | 0.25 | 0.50 | 0.29 | 2.32 |
| | | High-irrigation | 52 | | 0.31 | 0.50 | 0.38 | 2.45 |
| | Second | Control | 88 | 19.2±5.2 | 0.50 | 0.68 | 0.84 | 2.47 |
| | | Low-irrigation | 106 | | 0.61 | 0.68 | 0.94 | 2.27 |
| | | High-irrigation | 124 | | 0.72 | 0.68 | 1.16 | 2.37 |

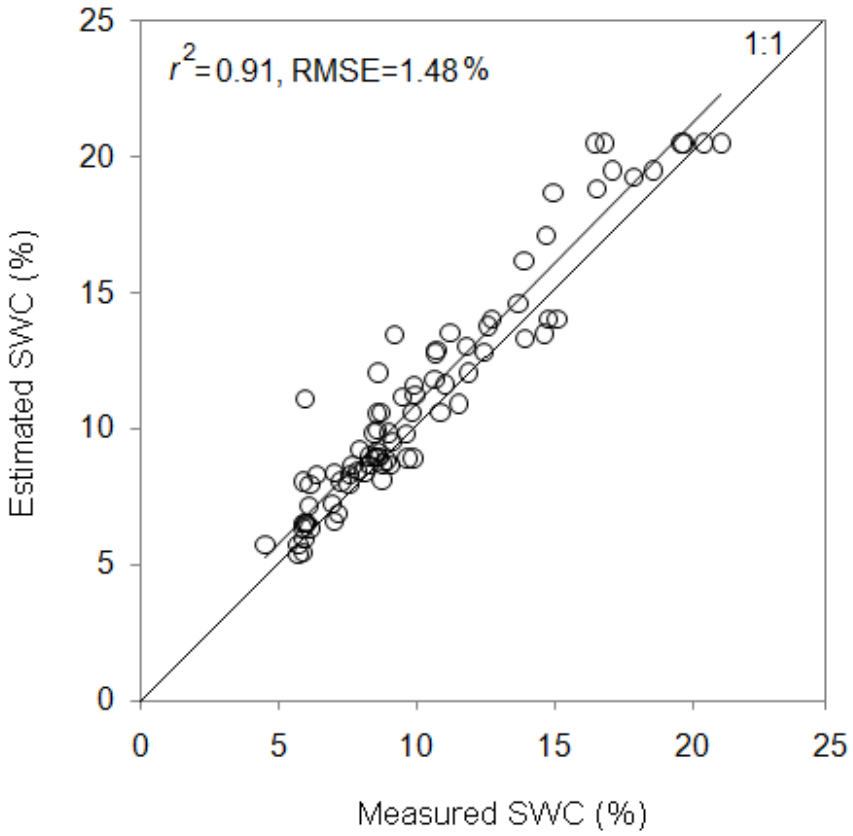


**Figure 4.5** Scatter diagram between the estimated SWC by the water balance model and measured SWC in 2009 and 2010.

During the observation period, daily average air temperature varied between 3.5 ºC (9 May) and 25.8 ºC (4 July) in 2009, and between 3.9 ºC (7 May) and 31.1 ºC (26 June) in 2010. Average temperature was significantly lower ($p < 0.05$) during the first period (15.8±5.4 ºC in 2009 and 16.4±6.6 ºC in 2010) than during the second period (19.8±2.7 ºC and 19.2±5.2 ºC).

Based on above seasonal differences of soil moisture and temperature conditions, the features of two periods were identified: the first period was dry and comparably colder whereas second period was wet and warmer in both years.

### 4.3.2 Vegetation growth

The two growing seasons were characterized by similar pattern of AGB and BGB; however the values were greater in 2009 than in 2010. AGB in all treatments did not differ significantly ($p > 0.05$) before irrigation (initial conditions on 25 May 2009 and 12 June 2010), but after the irrigation treatments commenced, AGB became significantly greater ($p < 0.05$) in the irrigated plots than in the control plots (Figures 4.6) Visible differences in plant growth under different water treatments were shown in Appendix D on page 83. At the final sampling in 2009, the maximum AGB values were 117, 218 and 316 g/m$^2$ for the control, low-irrigation, and high-irrigation plots, respectively (Figure 4.6a). Correspondingly, lower AGB (98, 132 and 185 g /m$^2$) was observed in 2010 (Figure 4.6b).

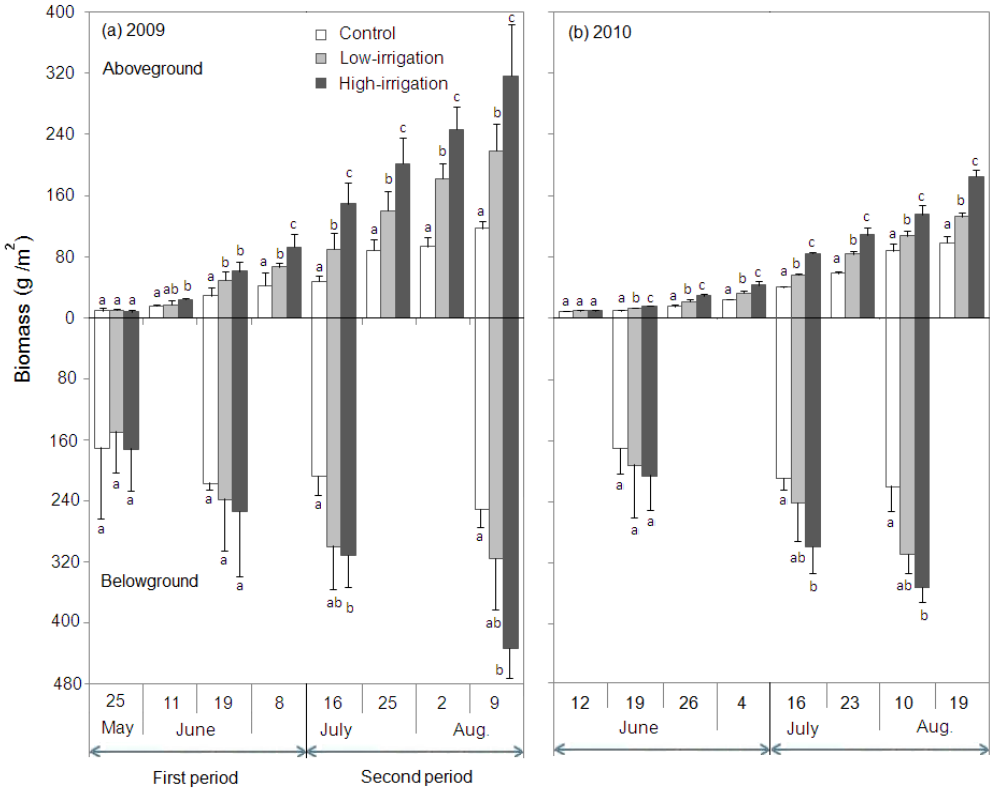


**Figure 4.6** Seasonal changes in AGB and BGB in the control and in the two water (irrigation) treatments in (a) 2009 and (b) 2010. Error bars represent standard deviations. Bars on a given date labeled with different letters differ significantly ($p < 0.05$) between the treatments. The first and second periods are denoted by horizontal arrows.

AGB at the final sampling in 2009 consisted of 11, 20, and 21% of perennial grasses and 89, 80, and 79% of annual grasses for the control, low-irrigation and high-irrigation plots, respectively (Table 4.2). However, AGB of perennial grasses was large in 2010 (40, 51, and 46% for the control, low- and high-irrigation plots, respectively. The percentages of perennial grasses in both the irrigated plots were significantly higher ($p < 0.05$) than in the control plot in both the years.

**Table 4.2** Plant species and their AGB ($g/m^2$) for C (Control), L (Low-irrigation) and H (High-irrigation) at the final samplings (at the time of peak biomass production) in 2009 and 2010. The mean represent the average value of the 4 replications while % indicate that percentages of each species from the total biomass.

| Life cycle | Species | 9 Aug 2009 | | | | | | 19 Aug 2010 | | | | | |
|---|---|---|---|---|---|---|---|---|---|---|---|---|---|
| | | C | | L | | H | | C | | L | | H | |
| | | Mean | % | Mean | % | Mean | % | Mean | % | Mean | % | Mean | % |
| Perennial | Agropyron cristatum | 0.2 | 0.1 | 0.2 | 0.1 | 0.6 | 0.2 | 4.0 | 4.1 | 8.6 | 6.5 | 18.1 | 9.8 |
| | Cleistogenes squarrosa | 1.9 | 1.6 | 6.8 | 3.1 | 18.3 | 5.8 | 0.7 | 0.7 | 10.2 | 7.8 | 6.7 | 3.6 |
| | Elymus chinensis | 3.0 | 2.5 | 2.4 | 1.1 | 7.1 | 2.2 | 12.0 | 12.3 | 10.6 | 8.1 | 13.7 | 7.4 |
| | Stipa Krylovii | 0.5 | 0.4 | 0.5 | 0.2 | 0.0 | 0.0 | 1.2 | 1.2 | 6.8 | 5.2 | 7.2 | 3.9 |
| | Carex korshinskii | 2.2 | 1.9 | 1.8 | 0.8 | 4.8 | 1.5 | 1.1 | 1.1 | 3.8 | 2.9 | 7.5 | 4.0 |
| | Artemisia Adamsii | 5.0 | 4.3 | 28.7 | 13.2 | 34.7 | 11.0 | 18.6 | 19.1 | 23.4 | 17.8 | 16.3 | 8.8 |
| | Artemisia Frigida | 0.1 | 0.1 | 1.0 | 0.4 | 0.2 | 0.1 | - | - | 1.3 | 1.0 | 10.0 | 5.4 |
| | Caragana spp | 0.6 | 0.5 | 2.9 | 1.3 | 1.0 | 0.3 | 1.5 | 1.5 | 2.1 | 1.6 | 5.9 | 3.2 |
| | **Total** | 13.5 | **11.5** | 44.3 | **20.3** | 66.6 | **21.1** | 39.0 | **40.1** | 67.0 | **50.8** | 85.3 | **46.2** |
| Annual | Bassia dasyphylla | 0.6 | 0.5 | 0.4 | 0.2 | 0.7 | 0.2 | - | - | - | - | - | - |
| | Chenopodium spp. | 14.6 | 12.4 | 31.5 | 14.5 | 46.6 | 14.8 | 0.3 | 0.3 | 0.2 | 0.2 | 0.5 | 0.3 |
| | Dontostemon integrifolia | 0.1 | 0.1 | 0.6 | 0.3 | 2.8 | 0.9 | - | - | - | - | - | - |
| | Salsola ruthenica | 88.5 | 75.5 | 141.2 | 64.8 | 199.6 | 63.2 | 58.5 | 60.1 | 64.7 | 49.0 | 98.9 | 53.5 |
| | **Total** | 103.8 | **88.5** | 173.7 | **79.7** | 249.7 | **79.0** | 58.3 | **59.9** | 64.9 | **49.2** | 99.4 | **53.8** |

The effect of the irrigation on BGB was not detected during the first period in both years; BGB in all treatments did not differ significantly ($p > 0.05$), while significant ($p < 0.05$) differences were obtained only between control and high-irrigation plots during the second periods (Figure 4.6). BGB was higher than AGB for all treatments. A ratio of BGB

to AGB (BGB:AGB) significantly increased ($p < 0.05$) in the control plots as compared with irrigated plots (Table 4.3).

**Table 4.3** A ratio of BGB to AGB for control, low-irrigation and high-irrigation plots in 2009 and 2010.

| Date | Control | Low-irrigation | High-irrigation |
|---|---|---|---|
| 19 June 2009 | 7.55 | 4.87 | 4.14 |
| 16 July 2009 | 4.33 | 3.35 | 2.08 |
| 9 Aug 2009 | 2.14 | 1.45 | 1.37 |
| 19 June 2010 | 18.44 | 15.16 | 13.24 |
| 16 July 2010 | 5.31 | 4.34 | 3.60 |
| 10 Aug 2010 | 2.53 | 2.90 | 2.63 |
| **Average** | **6.72** | **5.34*** | **4.51*** |

* The BGB:AGB are significantly lower at low and high-irrigation plots than control plots

### 4.3.3 Radiation interception and its relationship with NDVI and biomass

Increased water availability resulted in increased canopy radiation interception; *fIPAR* increased from 0.22 at the start of the study period to 0.27 at the end in the control, from 0.24 to 0.32 in the low-irrigation treatment and from 0.23 to 0.45 in the high-irrigation treatment in 2009 (Figure 4.7a). Similarly, *fIPAR* increased in 2010 (Figure 4.7b): 0.23–0.27, 0.24–0.32 and 0.23–0.36 for the control, low- and high-irrigation plots, respectively. The differences between the treatments were significant ($p < 0.05$) in 2009, while significant ($p < 0.05$) difference was obtained only between control and high-irrigation plots in 2010. In both years the average *fIPAR* was significantly higher ($p < 0.05$) during the second period than during the first period in the irrigated plots.

Similarly, at the end of growing season in 2009, the highest values of NDVI were 0.21, 0.25 and 0.31 for the control, low-irrigation, and high-irrigation plots, respectively, whereas they were relatively low (NDVI = 0.19, 0.21 and 0.26) in 2010. Thus, the

estimated NDVI provided a good linear estimates of *fIPAR* by natural vegetation ($r^2$ = 0.81, $p < 0.05$; Figure 4.8). A significant correlation was found ($r^2$ = 0.82, $p < 0.05$) between AGB and *fIPAR* (Figure 4.9).

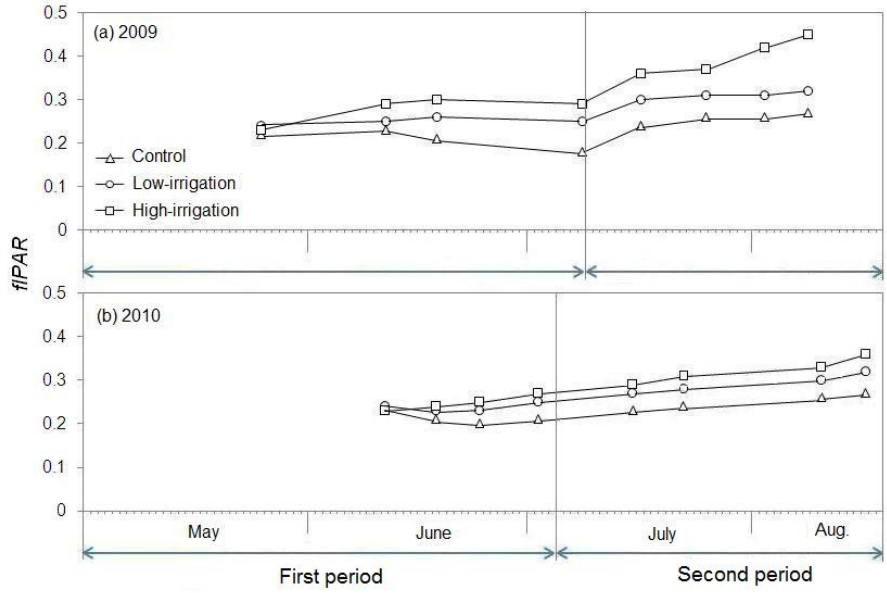


**Figure 4.7** Seasonal changes in the *fIPAR* in the control, low-irrigation, and high-irrigation plots in (a) 2009 and (b) 2010. The first and second periods are denoted by horizontal arrows.

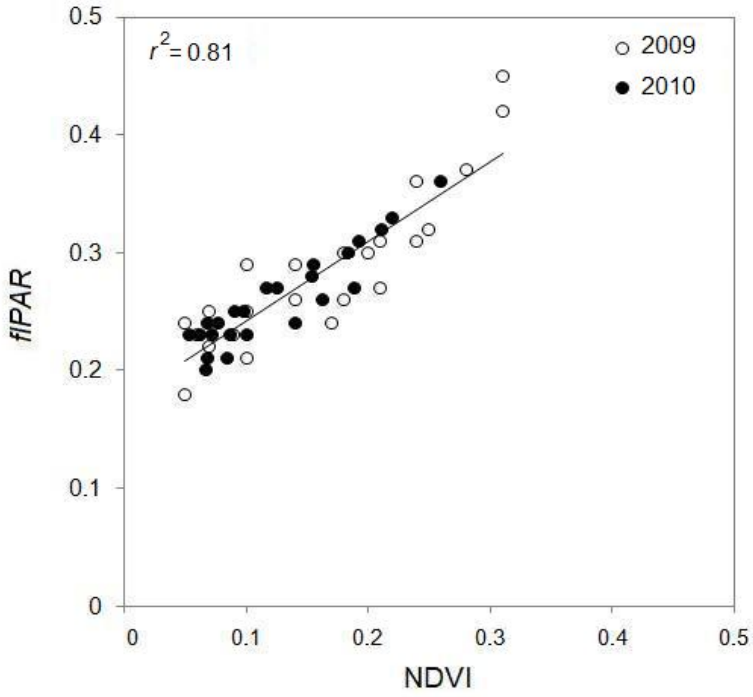


**Figure 4.8** Relationship between the *fIPAR* and the NDVI in 2009 and 2010.

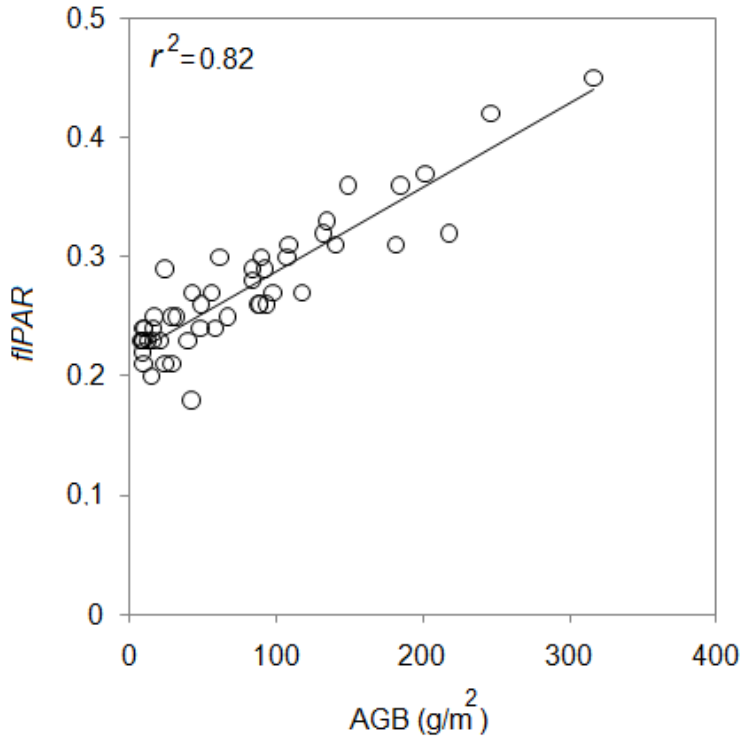


**Figure 4.9** Relationship between the *fIPAR* and AGB in 2009 and 2010.

### 4.3.4 Estimation of radiation use efficiency

Aboveground biomass was clearly different between the growth periods and also between the years (Figure 4.6). Therefore, to better describe RUE based on AGB ($\varepsilon_a$) in each treatment, two separate regression lines for the first and second periods were established (Figure 4.10). Due to the above-mentioned stress condition, $\varepsilon_a$ values during the first period were clearly low for all treatments, compared with the $\varepsilon_a$ values during the second period. A significant high correlation ($r^2$ = 0.93, $p$ < 0.05) was obtained between $\varepsilon_a$ and $f_{WS}$.

The temperature stress factor during the second period was comparably lower in 2010 ( $f_{TS} = 0.68$ ) than in 2009 ( $f_{TS} = 0.82$ ) (Table 4.1). For the control plot, $f_{WS}$ (0.20–0.56) was lower than $f_{TS}$ (0.50–0.82). Based on estimated $\varepsilon_a$, $f_{WS}$ and $f_{TS}$, determined

$\varepsilon_{MAX}$ was nearly constant (2.11–2.66 g AGB/MJ IPAR, averaging 2.34 g AGB/MJ IPAR) for various stress conditions during the growth periods of two years (Table 4.1).

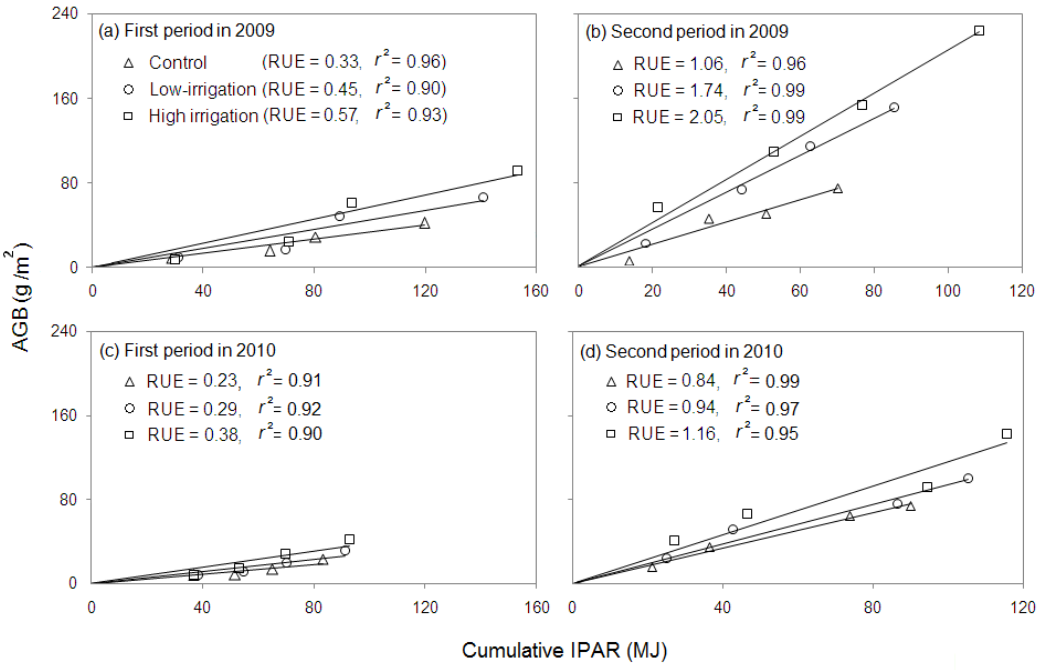


**Figure 4.10** Relationships between AGB and the cumulative IPAR during the first and second periods of 2009 (a, b) and 2010 (c, d). The slopes of the solid regression lines represent the RUE values for each treatment.

## 4.4 Discussion and conclusions

The BGB was several times higher than AGB (Figure 4.6). This generally agreed with the results reported by the previous studies for perennial native ecosystems in the arid and semi-arid regions (Coleman, 1976; Shinoda *et al*., 2010b). It is attributed to large BGB at the beginning of the growing season; the biomass could include the roots and underground stems of perennials from the previous season and pre-season BGB before the aboveground growth began.

The BGB:AGB also increased with the increase of water stress, indicating that the aboveground growth was affected more severely than the belowground growth. This could be explained by the osmotic adjustment, which leads to enhanced allocation to roots (e. g., Kramer, 1983; Wilson, 1988).

Canopy radiation interception generally increased throughout the growing season due to increased leaf area. In this study, however, the radiation interception decreased (in the control and low-irrigation plots) from mid June to early July in 2009 (Figure 4.7a) and from mid June to late June in 2010 (Figure 4.7b). This could result from soil water depletion due to low precipitation (totaling 7 and 3 mm during the above periods, respectively) (Figure 4.4). Since the leaves temporarily wilted or rolled under the water stress, the radiation interception ability led to being decreased, as observed in the field. In general, the stomata on the leaves tend to close under water stressed condition in order to limit transpiration and prevent wilting (Comstock and Ehleringer, 1993). Therefore, closing of the stomata may also cause limitation of radiation interception under such a dry condition. The results of the present study agree with the previous studies on crop radiation interception under water stress (Blum, 1996; Tesfaye *et al*., 2006).

The previous studies demonstrated that a vegetation index based on remote sensing data can be used as an indicator of APAR, which is a key parameter in many PEMs (Sellers, 1987; Goward and Huemmrich, 1992). In the present study, significant linear relationship between *fIPAR* by natural vegetation and estimated NDVI was obtained. This indicates that NDVI, based on field-measured irradiance data, is an important tool for deriving *fIPAR* in the study area.

To test the validity of reported relationship between *fIPAR* and NDVI, *fIPAR* based on linear estimations of the CASA and GLO-PEM models were compared with the measured *fIPAR*. The CASA underestimates *fIPAR*

( $fIPAR_{CASA} = 0.88 \times fIPAR_{measured} - 0.17$, $r^2$ = 0.84, $p < 0.05$, RMSE = 0.2), whereas the GLO-PEM underestimates and overestimates *fIPAR* for its low and high values, respectively ( $fIPAR_{GLO-PEM} = 1.99 \times fIPAR_{measured} - 0.38$, $r^2$ = 0.81, $p < 0.05$, RMSE = 0.13). Thus, the model calibrations are needed in both the models for the accurate estimation of *fIPAR* by green vegetation for the specific region.

Leaf area index is a key parameter that determines radiation interception. However, the measurement of LAI is labor-intensive and time-consuming, especially for small grasses with thin leaves. On the other hand, although green leaves are the dominant photosynthetic organ in most plants, there is evidence that nonfoliar organs such as greenish flowers or developing fruits (Weiss *et al*., 1988; Blanke and Lenz, 1989), stem tissues (Nilsen, 1995), and even roots (Hew *et al*., 1984) can be photosynthetically active (Aschan and Pfanz, 2003). Among these alternative photosynthetic organs, stem photosynthesis can make a major contribution to whole-plant carbon gain (Nilsen, 1995), particularly during periods of environmental stress (Nilsen and Bao, 1990). Therefore, in this study it was assumed that not only green leaves but also green nonfoliar organs such as stems and flowers (which were included in AGB) contribute to carbon gain. This decision was made because some of the grass species at the study site, such as S. krylovii and A. cristatum are leafless and also most grasses in there consist primarily of green leaves and stems. As expected, a significant correlation ($r^2$ = 0.82, $p < 0.05$) between AGB and *fIPAR* was found (Figure 4.9). This demonstrated that the nonfoliar organs were also important for carbon acquisition. Thus, the relationship between AGB and *fIPAR* can be used instead of the relationship between LAI and *fIPAR* to represent the extinction coefficient in canopy radiation-transfer models (e.g., Monsi and Saeki, 1953) for such grasslands.

RUE values for natural grasslands have been poorly documented and may not be strictly comparable in different grasslands because of differences in the vegetation and climatic conditions. To provide units that would be comparable with those in other studies, the biomass values was converted into carbon (C) equivalents using 0.45 g C per gram of dry matter for the grass and foliage components (Raich *et al*., 1991). IPAR and APAR are often used interchangeably in the dry regions, although IPAR is slightly higher than APAR because a small fraction of PAR is reflected by green leaves (Gallo and Daughtry, 1986). The estimated RUE based on AGB during the first periods (0.15 g C AGB/MJ IPAR in 2009 and 0.10 g C AGB/MJ IPAR in 2010) were similar to the value of 0.13 g C ANPP/MJ IPAR for the semi-arid grassland in southeastern Arizona (Nouvellon *et al*., 2000) and the values of 0.1 g C ANPP/MJ APAR for less-productive sites and 0.2 g C ANPP/MJ APAR for the most productive sites at 19 grassland sites in the central United States (Paruelo *et al*., 1997). The estimated RUE during the second periods (0.48 g C AGB/MJ IPAR in 2009 and 0.38 g C AGB/MJ IPAR in 2010) were equivalent to RUE reported by (Hanan *et al*., 1995) and (Mougin *et al*., 1995) (0.36 and 0.46 g C ANPP/MJ IPAR, respectively, for annual grassland in the Sahel). The previous studies have reported that RUE with low water availability is less than that with high water availability in grassland ecosystems (Nouvellon *et al*., 2000; Hunt *et al*., 2002). In the present study differences in estimated RUE between the two periods and also between the years were explained primarily by the soil water conditions. In addition to the water stress, low temperatures during the first period had an adverse effect on estimated RUE. Nakano *et al*. (2008) indicated that within the temperature range of 14–38ºC, CO2 uptake was 90% of the maximum value in the study area, as stomata could remain more open at higher temperatures than at lower temperatures (Correia *et al*., 1999). In the present study high levels of temperature stress ( $f_{TS} \leq 0.36$ ) mainly resulted from low temperatures (<14ºC).

The strong dependence of RUE on SWC and air temperature, especially in dry and cold regions like Mongolia, has also been reported (Potter *et al*., 1999).

Based on estimated RUE and water and temperature stress factors, the maximum RUE for the grassland ecosystem was determined. If the stress factors fully represent the environmental stress, maximum RUE should be similar among the various stress conditions. In this study, estimated maximum RUE values for the twelve cases (three water treatments × two different periods × two years) were nearly constant (Table 4.1), indicating that the stress factors well represented the water and temperature stresses. Also the maximum RUE value was estimated with the CASA sub-models for the water and temperature stresses. The high water stress (low value of $f_{WS}$) was obtained in the first periods ( $f_{WS}$ = 0.63, 0.68 and 0.74 for the control, low- and high-irrigation plots, respectively, in 2009 and $f_{WS}$ = 0.59, 0.61 and 0.66 in 2010), whereas correspondingly low water stress (relatively high value of $f_{WS}$) was found in the second periods ( $f_{WS}$ = 0.75, 0.94 and 0.97 in 2009 and $f_{WS}$ = 0.74, 0.83 and 0.90 in 2010). Similarly, the temperature stress was high (low value of $f_{TS}$) during the first periods ( $f_{TS}$ = 0.85 in 2009 and $f_{TS}$ = 0.81 in 2010) and low (relatively high value of $f_{TS}$) during the second periods ( $f_{TS}$ = 0.97 in 2009 and $f_{TS}$ = 0.88 in 2010). Including these stress factors in Equation (4.2), maximum RUE values of 0.46–2.17 g AGB/MJ IPAR were found. Thus, sub-models used for determining the stress factors are location-dependent, and further studies will be needed to develop the sub-models that can be employed for regional-scale NPP simulation.

Based on the results, the following main conclusions were obtained: (1) RUE responded rapidly to changes of water availability and seasonal temperature; (2) The equations used for water and temperature stresses were useful to represent the

environmental conditions in the dry region; and (3) The comparison of water and temperature stresses on estimated RUE demonstrated that water stress had stronger effect in reduced RUE. This study is one of the few experimental studies that estimate RUE for natural grasslands in response to different water and temperature conditions. Results from this study, therefore, provide an important basis for improving radiation-based NPP models that can be used in semi-arid regions.

# CHAPTER 5

## Estimation of pasture productivity in Mongolian grasslands[2]

## 5.1 Introduction

Considering the large area of Mongolia, it is difficult to monitor vegetation conditions widely. Modeling is an important approach to improve our understanding of the vegetation dynamics. In Mongolia, progress in estimating and modeling the carbon cycle of grassland ecosystems has been seriously limited. Nakano *et al*. (2008) measured $CO_2$ fluxes both inside and outside of a site of drought experiment that was conducted at Bayan Unjuul in Mongolia (Shinoda *et al*., 2009), using a closed-chamber technique. They

[2] This chapter is edited version of

Tserenpurev Bat-Oyun, Masato Shinoda, Mitsuru Tsubo (2010), Estimation of pasture productivity in Mongolian grasslands: field survey and model simulation. *Journal of Agricultural Meteorology*. 66 (1): 31–39.

demonstrated that the reduction of gross primary production (GPP) per unit AGB (GPP/AGB) was caused by a combination of high vapor pressure deficit and low soil moisture. Bolortsetseg (2006) analyzed the effects of climate change on AGB in Mongolia using the Century model (namely, a model designed to simulate carbon, nutrient, and water dynamics for different types of ecosystems including grasslands). The sensitivity analysis indicated that AGB was more sensitive to changes in precipitation than those in temperature.

A number of models have been developed to simulate productivity of different ecosystems; among these the PEM was selected, because it does not include complex ecophysiological parameters. In origin, Monteith (1972) explored that primary production was linearly related to the amount of radiation received by plant stand. Later, this approach was theoretically and experimentally strengthened (Monteith, 1977); as a result, it has become the most commonly used method of analyzing and modeling plant growth. It has been found that a remote-sensing-based vegetation index is an indicator of APAR by green vegetation (Sellers, 1987; Sellers *et al.*, 1992; Goward and Huemmrich, 1992). In the model, the *fIPAR* is estimated from NDVI data. Several studies have evaluated the performance of the PEM for various regions. For instance, the CASA model successfully simulated the spatial and temporal distribution of NPP in northern China using MODerate Resolution Imaging Spectroradiometer (MODIS) data (Yuan *et al.*, 2006), interannual variations of cropland NPP in the United States (Lobell *et al.*, 2002), and maize production across China (Tao *et al*., 2005). However, there have been very few attempts to apply this kind of model to Mongolia. Given this background, this study aims to estimate pasture productivity; and investigate climatic effect on pasture productivity in Mongolia using the PEM based on satellite data.

## 5.2 Materials and methods

### 5.2.1 Study sites

Figure 5.1 illustrates four study sites; Mandalgovi (45.77°N, 106.28°E, desert steppe), Bayan Unjuul (47.04°N, 105.95°E, dry steppe*), Darkhan (49.47°N, 105.98°E, steppe), and Bulgan (48.80°N, 103.55°E, forest steppe) located in three vegetation zones of Mongolia. The growing season for the grasslands is very short (April–September, depends on region) and is limited by low temperature and precipitation. In particular, moisture availability is generally considered the most important determinant for vegetation growth and the large seasonal variations in precipitation are clearly reflected in plant growth (Gunin *et al*., 1999).

In general, precipitation decreases and temperature increases from the north to south, resulting in warmer and more arid conditions in the south. Average (1995–2007) air temperature at the Institute of Meteorology and Hydrology (IMH) station was 14.4 °C at Mandalgovi, 14.3 °C at Darkhan, 13.8 °C at Bayan Unjuul and 11.8 °C at Bulgan during the growing season. Average precipitation during the growing season was low at Mandalgovi (124 mm) and Bayan Unjuul (135 mm) and high at Darkhan (268 mm) and Bulgan (291 mm). It should be noted that the study years (2005–2007) were among the driest years during 1995–2007 for the study sites except for Darkhan.

Plant composition varies among the different ecosystems. The Bulgan and Darkhan sites are co-dominated by *Stipa krylovii*, *Agropyron cristatum*, *Cleistogenes squarrosa*, *Leymus chinensis*, and *Carex* spp., while Mandalgovi is co-dominated by *Stipa krylovii*, *Cleistogenes squarrosa*, *Allium polyrrhizum*, and *Artemisia frigida* (Bolortsetseg *et al*., 2002). The Bayan Unjuul site is co-dominated by perennial grasses such as *Stipa krylovii*, *Agropyron cristatum*, and *Cleistogenes squarrosa*, by forbs such as *Artemisia adamsii* and

*Chenopodium aristatum*, and by small shrubs (*Caragana* spp.) (Shinoda *et al*., 2009, Appendix C on pages 80−82).

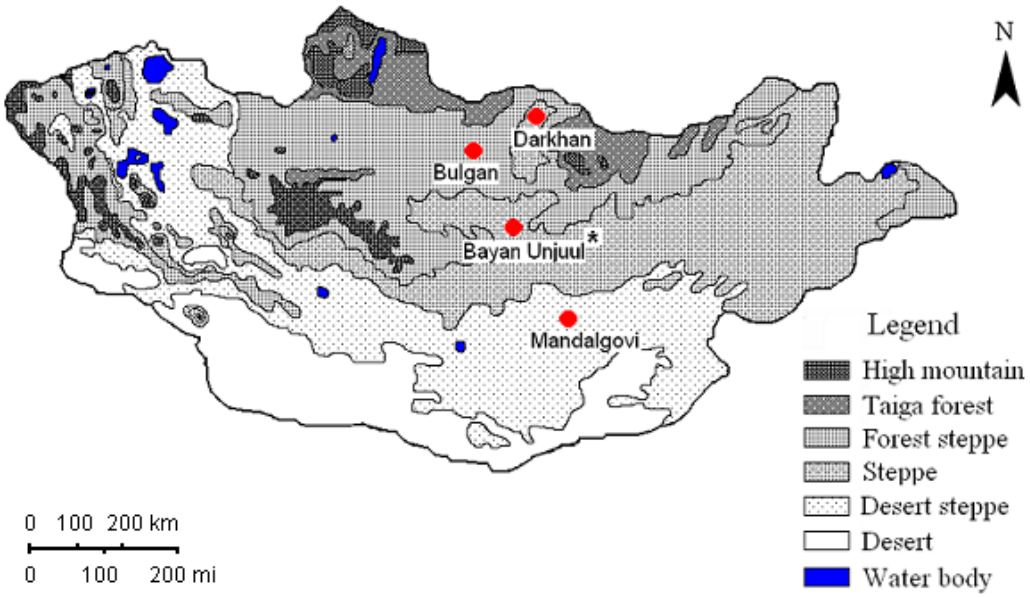


**Figure 5.1** Locations of study sites in vegetation zone map of Mongolia. *Bayan Unjuul situated at steppe vegetation zone, although it in transition between steppe and desert steppe under drier condition as compared with Darkhan at steppe. Therefore, in order to distinguish from Darkhan, in this chapter it was referred by dry steppe site.

## 5.2.2 Data

Data used for this study were provided by IMH of Mongolia. The data included climate (temperature, precipitation, and solar radiation), soil moisture, soil texture and AGB in grazing plots for Darkhan, Bulgan, Bayan Unjuul and Mandalgovi during the growing season of 2005–2007. The IMH measured animal-available AGB (located above the 1-cm height of grasses from the ground surface) in four 1-$m^2$ plots at each of the three study sites (Darkhan, Bulgan, and Mandalgovi) at monthly intervals for grazing plots. Unlike at the other stations, the clipping of AGB for Bayan Unjuul was conducted at the

ground level. The procedure included clipping, drying and weighing the dried AGB. Aboveground biomass was expressed as dry matter weight per unit area ($g/m^2$). To compare the measured AGB with simulated results, biomass values were converted into carbon (C) equivalents using the ratio of 0.45 (for grass and foliage components) as the mass of C per gram dry mass (Raich *et al*., 1991).

Sixteen-day composite MODIS NDVI images with the highest resolution (250m×250 m) were obtained from the Earth Observation System data gateway (**https://wist.echo.nasa.gov/api/**). The products were corrected atmospherically, considering ozone absorption and molecular scattering.

### 5.2.3 Model description

The model's NPP component is based on the concept of radiation-use efficiency described by Monteith (1972, 1977). Flowchart of ANPP calculation is shown in Figure 5.2.

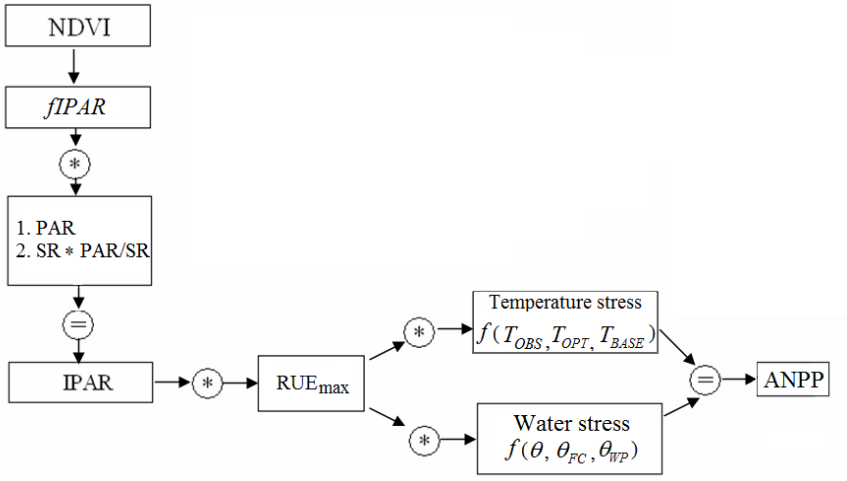


**Figure. 5.2** The flowchart of the NPP model algorithm used to estimate ANPP. The model has three key inputs: 1. remote sensing input NDVI, used to derive *fIPAR*, 2. meteorological inputs (PAR, which is used to estimate IPAR based on *fIPAR*; average temperature ($T_{OBS}$), base

temperature ($T_{BASE}$) and optimum temperature ($T_{OPT}$) which are used to estimate temperature stress factor ( $f_{TS}$ ); and soil water content ($\theta$), soil water content at field capacity ($\theta_{FC}$) and soil water content at wilting point ($\theta_{WP}$) which are used to calculate water stress factor ( $f_{WS}$ )) 3. biome-specific coefficient (RUE). RUE is used with the IPAR to estimate ANPP.

ANPP is estimated from total *PAR* (MJ/m$^2$/month), *fIPAR*, and *RUE* as expressed by the following equation:

$$ANPP = PAR \cdot fIPAR \cdot RUE \tag{5.1}$$

where *fIPAR* is calculated by CASA submodel (as a linear relationship between *fIPAR* and simple ratio (*SimR*), slope and intercept were adjusted (Sellers, 1993)). *SimR* is given by:

$$SimR(x,t) = [1 + NDVI(x,t)]/[1 - NDVI(x,t)] \tag{5.2}$$

where *x* represents the grid cell and *t* represents the month. *fIPAR* is calculated as:

$$fIPAR(x,t) = \min\{SimR(x,t)/[SimR_{\max} - SimR_{\min}] - SimR_{\min}/[SimR_{\max} - SimR_{\min}], 095\} \tag{5.3}$$

where $SimR_{\max}$ approximates the *SimR* value at which all incident solar radiation is intercepted and it corrects the effects of canopy architecture and residual cloud contamination. This value is set to 5.13 for grasslands. $SimR_{\min}$ represents the *SimR* value for unvegetated land areas and is set to 1.08 for all grid cells. A cap of 0.95 was imposed on *fIPAR* in order to reflect a finite upper limit to leaf area. Thus, if *fIPAR* is greater than 0.95, *fIPAR* is set to 0.95 in equation (3).

The methodologies for estimation of IPAR, RUE and water and temperature stress factors were given in chapter 4. The PAR/SR was determined as a 0.438 during April–September (Chapter 3) while the maximum RUE was determined as a 2.34 g AGB/MJ IPAR (1.05 g C AGB/MJ IPAR) in Bayan Unjuul (Chapter 4). Therefore for the calculation of IPAR and RUE above determined values were used.

### 5.2.4 NDVI image processing

Moderate-resolution Imaging Spectroradiometer (MODIS) is a key instrument aboard the Terra (EOS AM) (Figure 5.3) and Aqua (EOS PM) satellites. Terra's orbit around the Earth is timed so that it passes from north to south across the equator in the morning, while Aqua passes south to north over the equator in the afternoon. Terra MODIS and Aqua MODIS are viewing the entire Earth's surface every 1 to 2 days, acquiring data in 36 spectral bands, or groups of wavelengths (see MODIS Technical Specifications). Description about the instrument is shown in Table 5.1.

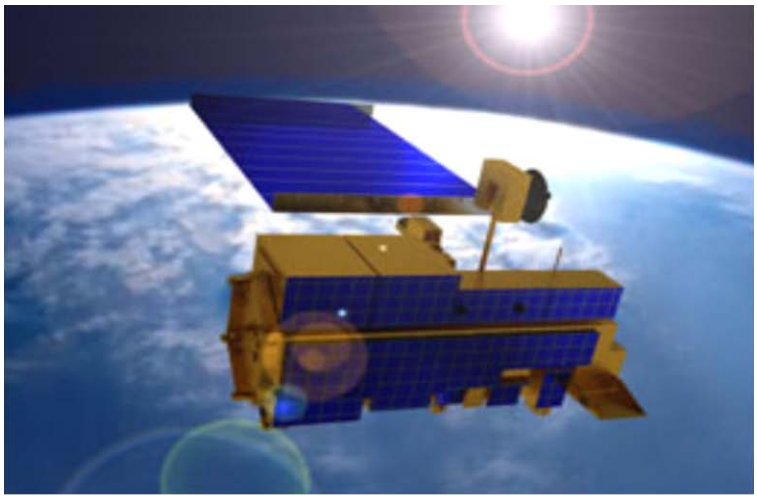

Fig. 2.1 MODIS TERRA sensor, *Source: MODIS Web*

**Figure 5.3** MODIS TERRA sensor, Source: MODIS Web (http://terra.nasa.gov/About/)

**Table 5.1** MODIS Instrument Description, *Source: MODIS Web*

| **Parameters** | **Value** |
|---|---|
| Orbit | 705 km, 10:30 a.m. descending node (Terra) or 1:30 p.m. ascending node (Aqua), sun-synchronous, near-polar, circular |
| Swath | 2330 km (cross track) by 10 km (along track at nadir) |
| Spatial resolution | 250 m (bands 1-2)<br>500 m (bands 3-7)<br>1000 m (bands 8-36) |
| Viewing angle | 0 ± 55 degrees of nadir |

In this analysis, MODIS NDVI images were reprojected from original Sinusoidal (SIN) projection to more standard geographic map projection. The pixel values of the four nearest neighbors that were obtained using bilinear algorithm were averaged. NDVI images observed in grazing area were used to estimate ANPP of grazing plots.

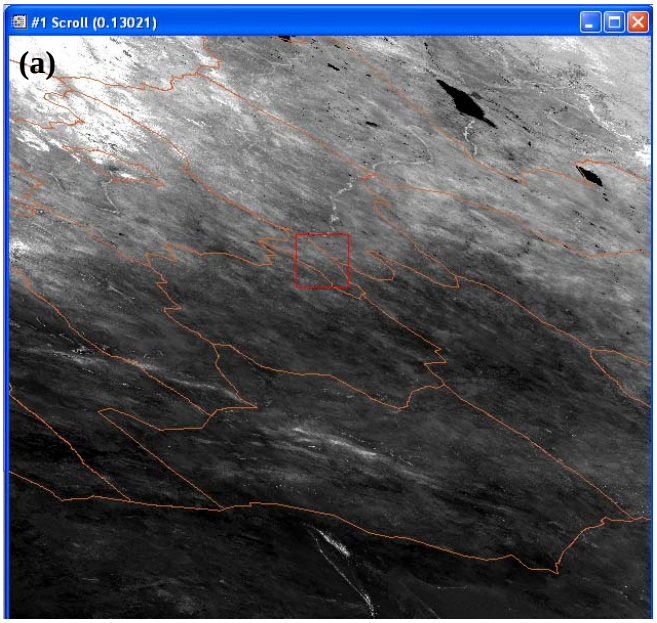

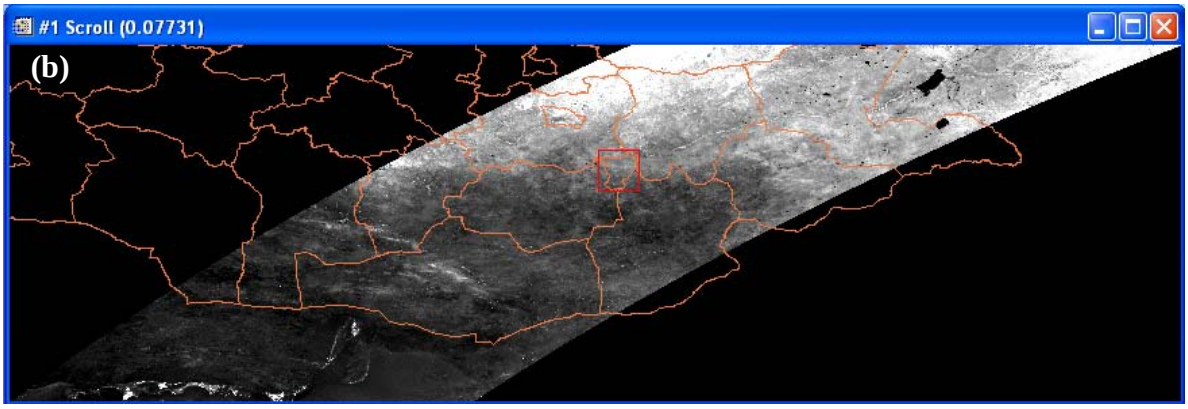


**Figure 5.4** (a) Original projection of MODIS NDVI image (b) Reprojected NDVI image into Geographic map projection

### 5.2.5 Simulation scenarios

In order to reveal the sensitivity of simulated ANPP under various climatic conditions, simulations were performed by changing stress conditions at four stress levels; no stress (control excluding all the stresses), temperature stress (water stress excluded), water stress (temperature stress excluded), and both the temperature and water stresses (actual conditions including all the stresses). Next, the relative contribution of each stress on ANPP was quantitatively estimated for the four study sites.

## 5.3 Results

### 5.3.1 Model simulation

Data from the four sites were analyzed to evaluate the effectiveness of model estimation of ANPP for the different vegetation zones. The spatial pattern of simulated ANPP (Figure 5.5) was similar to that of measured AGB (in Chapter 2, section 2.3.2), with the Darkhan (steppe) and Bulgan (forest steppe) sites most productive and Bayan Unjuul (dry steppe) and Mandalgovi (desert steppe) less productive. The high values of

simulated cumulative ANPP during the growing season (actual condition considering all the stress factors) were 68.2 and 45.8 g C/$m^2$ for Darkhan (Figure 5.5c) and Bulgan (Figure 5.5d), respectively, while low values were 16.6 and 6.9 g C/$m^2$ for Bayan Unjuul (Figure 5.5b) and Mandalgovi (Figure 5.5a), respectively.

Responses of ANPP to various stress levels were tested over the different vegetation zones, using the model output from 2005 to 2007. As expected from the latitudinal climatic gradient, water stress was relatively low for Bayan Unjuul and Mandalgovi, compared with Darkhan and Bulgan, due to insufficient water while temperature stress was lower for Bulgan (Table 5.2).

**Table 5.2** Temperature stress and water stress at four sites from 2005 to 2007 (averaged over the growing season).

| Stress factors | Temperature stress | | | Water stress | | |
|---|---|---|---|---|---|---|
| Year | 2005 | 2006 | 2007 | 2005 | 2006 | 2007 |
| Mandalgovi (desert steppe) | 0.48 | 0.46 | 0.54 | 0.31 | 0.33 | 0.29 |
| Bayan Unjuul (dry steppe) | 0.47 | 0.46 | 0.53 | 0.19 | 0.16 | 0.15 |
| Darkhan (steppe) | 0.47 | 0.44 | 0.52 | 0.44 | 0.45 | 0.40 |
| Bulgan (forest steppe) | 0.34 | 0.30 | 0.39 | 0.57 | 0.50 | 0.48 |

Cumulative ANPP over the growing season was reduced by 52–55% due to the temperature stress and by 83–84% due to the water stress for Bayan Unjuul and Mandalgovi, whereas for Bulgan and Darkhan, temperature and water stresses decreased ANPP by 45–58% and 62–65% of the control, respectively. These results demonstrate that at all the sites; water was the primary factor that influenced ANPP (Figure 5.5).

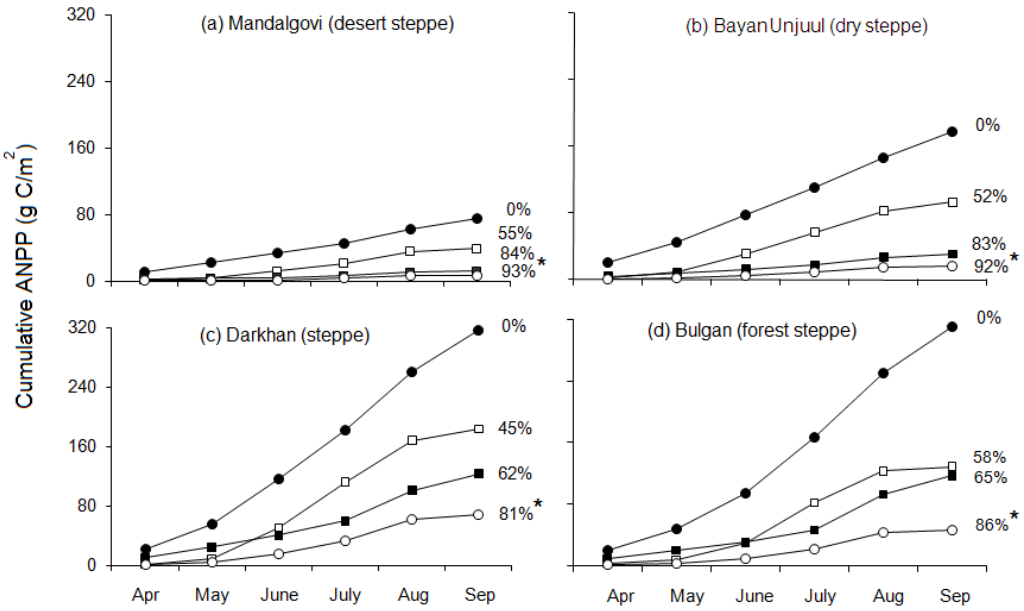


**Figure 5.5** Simulated cumulative monthly ANPP (average of 2005–2007) from four separate runs: —●— - no stress, —□— - temperature stress, —■— - water stress, —○— - temperature and water stress over the four sites. Percentage to the right of each line shows the relative decrease over growing season compared to the control. The asterisk denotes actual condition of grassland productivity.

The simulated ANPP was compared with the field-measured AGB at the four sites. Simulated cumulative ANPP from April to August was similar to AGB in August (time of peak biomass) for Mandalgovi and Bayan Unjuul, while it larger than the AGB for Darkhan and Bulgan (Figure 5.6).

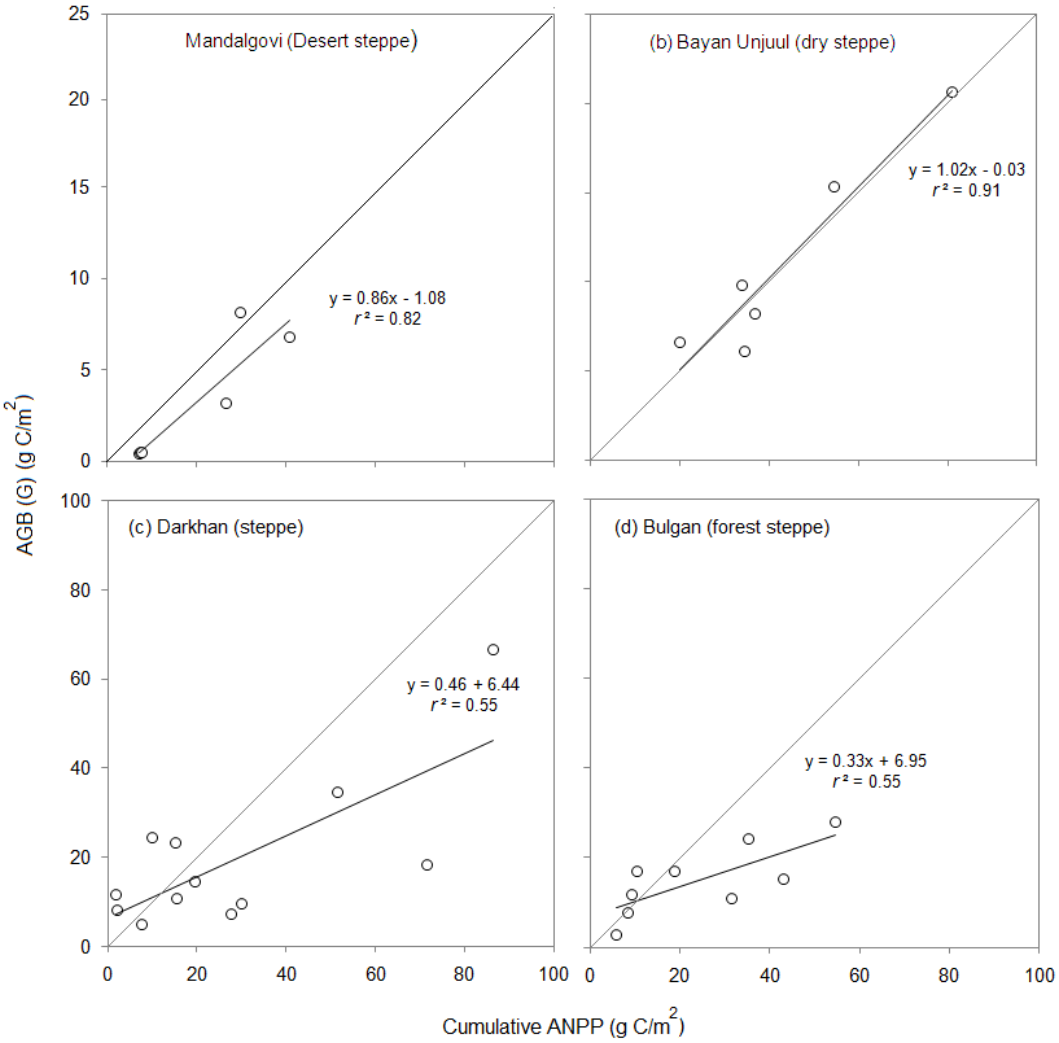


**Figure 5.6** Scatter diagram between the measured aboveground biomass at grazing plot AGB (G) and simulated cumulative ANPP at grazing plot from 2005 to 2007 for four sites.

## 5.4 Discussion and conclusions

Potter *et al.* (1993) simulated annual NPP using the CASA model and it was estimated as 28 g C $m^{-2}$ $yr^{-1}$ for desert and 180 g C $m^{-2}$ $yr^{-1}$ for perennial grasslands. On the other hand, the Century model estimated annual NPP of 27 g C $m^{-2}$ $yr^{-1}$ for the desert, 100 g C $m^{-2}$ $yr^{-1}$ for the steppe, and 290 g C $m^{-2}$ $yr^{-1}$ for the forest of Inner Mongolia and Mongolia (Chuluun and Ojima, 2002)). The simulated ANPP values in the Mongolian grasslands were substantially lower than those estimated by the above studies; this because

firstly, it is productivity of only aboveground part, secondly, the study years were among the driest years during 1995–2007.

The comparison between the measurements of AGB and simulation of ANPP indicated that simulated ANPP was similar with measured AGB for the desert steppe and dry steppe sites, whereas it tended to overestimated actual AGB for the steppe and forest steppe sites. Overestimation of ANPP due to; firstly, water and temperature stress factor that used for Bayan Unjuul was not applicable for Darkhan and Bulgan to represent environmental stresses; secondly, ANPP takes into account green biomass and also the litter (dead matter); thirdly, animal-available AGB (leaving 1-cm height of grasses from the ground surface) is a slightly underestimate of the total AGB.

Also, it should note that soil nutrient and species composition can affect on maximum RUE; however the effect of nutrient may small for the natural grassland whereas the effect of species composition is difficult to consider for mixed (consisted from many different species) natural grassland.

From the above-mentioned results, the following main conclusions were obtained:

1. The PEM simulated, reasonably well, the spatial variation of ANPP in the Mongolian grasslands. The simulated ANPP differed substantially from one vegetation region to another.
2. The analysis of effects of temperature and water stresses on pasture productivity demonstrated that water stress is stronger down-regulator of ANPP in the Mongolian grasslands.
3. Comparison of simulated ANPP and measured AGB indicated that simulated ANPP was similar with measured AGB for the desert steppe and dry steppe sites, whereas it tended to overestimated actual AGB for the steppe and forest steppe sites. Therefore, further model modification should be required for the steppe and forest steppe regions.

# CHAPTER 6

## General Conclusions

This research has provided an important insight into the following topics: (1) the effects of precipitation and grazing on pasture productivity, (2) quantification of PAR/SR, (3) quantification of RUE, and (4) estimation of pasture productivity using quantified parameters in the model.

Both precipitation and grazing have been shown to play important roles in determining pasture productivity; this conclusion is consistent with the findings of previous studies, which have identified a link with inter-annual changes in plant growth. Thus, in future, not only precipitation amount and event size, but also intensity and duration, should be considered to determine the impact of this variable on plant growth. Grazing effect on pasture productivity also indicates a link between species composition and total biomass. This has important implications for livestock production, and further research should therefore be undertaken to test this hypothesis.

PAR/SR has been reported from many sites; however, few studies have examined dry regions, including Mongolia. Based on the radiation dataset recorded at Bayan Unjuul, the annual PAR/SR (0.434±0.013) and growing season (April–September) PAR/SR (0.438±0.013) were determined. The effects of sky condition on this parameter were investigated, and it was found it that PAR/SR varied according to the clearness index, PAR/SR increased as the clearness index decreased, as sky conditions varied from clear to cloudy. This result is in agreement with previous studies and suggests that clearness index and water vapor pressure are the most important variables in determining PAR/SR.

Accurate estimation of RUE is essential for modeling plant productivity, but limited information is available for dry grassland. RUE was quantified based on direct field measurements of radiation interception and AGB, and these data were collected eight times during the growth period in 2009 and 2010. The maximum RUE was found to be 1.05±0.16 g C AGB/MJ IPAR by excluding the effects of water and temperature stresses while RUE varied widely (0.10–0.48 g C AGB/MJ IPAR) under negative correlation with soil water and low temperature stresses. Russell *et al*. (1989) reported that RUE varies over a relatively narrow range for crops but over a wider range for natural ecosystems, because these have a greater variety of environmental stresses. Based on field measurements, the quantified RUE for dry periods in 2010 and 2009 (0.10 g C AGB/ MJ IPAR and 0.15 g C AGB/ MJ IPAR, respectively) were similar to values obtained in southeastern Arizona (Nouvellon *et al*., 2000) and in central USA (Paruelo *et al*., 1997). However, the values during wet periods of these two years (0.38 g C AGB/ MJ IPAR and 0.48 g C AGB/ MJ IPAR) were equivalent those of annual grassland habitats in the Sahel (Hanan *et al*., 1995; Mougin *et al*., 1995).

To examine the suitability of the PEM, ANPP was estimated for different sites in distinct vegetation zones. A comparison between measurements and simulation results indicated that simulated ANPP was similar to measured AGB for the Mandalgovi and Bayan Unjuul sites, whereas it tended to over-estimate actual AGB for the Darkhan and Bulgan sites, where the climate is wetter and colder. Over-estimation of ANPP suggests that, first, the sub-models used for determining stress factors may be location-dependent and that further studies are needed to develop these sub-models to ensure they can be employed to estimate NPP at the regional scale. For example, it is necessary to take into account plant physiological characteristics, such as base and optimum temperatures, which can vary from region to region. Second, ANPP takes into account litter (i.e., dead matter),

and in Mandalgovi and Bayan Unjuul the proportion of this is small, whereas Darkhan and Bulgan litter may should not be neglected. It suggests that for the model validation quantity of litter production need to be adjusted according to the location (vegetation zone). Third, LAI in the height range 0–1 cm accounts for approximately 10% of the total for the forest steppe and steppe sites (Nachinshonhor, 2001). This result suggests that animal-available AGB slightly underestimates the total AGB at Darkhan and Bulgan.

Based on the findings outlined above, the key outputs from this thesis can be summarized as follows.

- An analysis of the relationship between AGB and precipitation has improved our understanding of the responses of grassland productivity to changes in precipitation parameters.
- PAR/SR was quantified for a dry region at high latitude; this method can be used to obtain important parameters of PAR for dry regions, where SR data are available.
- In this study, the maximum RUE of 2.34±0.16 g AGB/MJ IPAR was quantified (by excluding the effects of water and temperature stresses) under various levels of seasonally varying water and temperature conditions during the growth period of two years: this value can be used in radiation-based models for dry regions. This is the first time that RUE has been quantified based on field measurements from the natural grasslands of Mongolia, and it is one of few assessments of RUE for natural grasslands worldwide.
- A simple radiation based model used in this study was applicable to dry regions in Mongolia to estimate pasture productivity.
- Overall, this study therefore provides an important basis for improving radiation-based ANPP models for use in dry regions of the world.

# SUMMARY

Mongolia is a country of nomadic livestock husbandry and its economy is dependent on livestock products. Natural grasslands are the main source of forage for these animals, and grassland productivity is strongly influenced by the country's dry, continental climate. The production of natural grassland is regulated by many factors, such as soil moisture, temperature, solar radiation, soil nutrient availability, and grassland utilization and management. Of these, soil moisture is the most critical and limiting factor determining the efficiency of plant radiation utilization and vegetation productivity in the country. A drying trend has recently been observed in soil moisture, further limiting pasture growth. This background emphasizes the importance of gathering accurate and timely information about pasture productivity for livestock survival. However, direct measurements can be difficult to gather, especially in remote areas of a large country like Mongolia. It is therefore essential to develop and validate models against observed measurements to estimate pasture productivity widely. The main aims of this thesis were to quantify input parameters (PAR/SR: the ratio of photosynthetically active radiation to solar radiation; and RUE: radiation use efficiency) of Production Efficiency Model (PEM) and to examine the suitability of PEM modified using the quantified parameters to estimate pasture productivity in the following vegetation zones: desert steppe, dry steppe, steppe, and forest steppe. A list of the main findings from this study given below:

First, the relationships between aboveground biomass (AGB) and precipitation were revealed. In this analysis, datasets for 15 sites were used, spanning the years 1986–2005. The results demonstrated that cumulative precipitation during the growth period had the highest significant correlation with AGB. When considered on a monthly basis, these data showed that precipitation in June had the most significant impact on AGB in forest

steppe, whilst precipitation in July was most significant in desert steppe and steppe zones. Moreover, at the desert steppe sites, where conditions are relatively dry, precipitation was strongly correlated with AGB, independent of event size, and even small precipitation events (≤ 5 mm) significantly affected AGB. Conversely, in the steppe and forest steppe zones, where conditions are relatively wet, AGB did not alter at small precipitation events, whereas large precipitation events (≥ 5.1 mm) tended to contribute to plant growth. This result suggests that more frequent and small precipitation events do not benefit vegetation growth in steppe and forest steppe zones. The results of this study provide an important contribution to experimental studies on the water requirements of natural grassland.

Second, the input parameter of PAR/SR for the PEM was quantified at Bayan Unjuul. The lowest monthly ratio occurred in April and December (0.42), while the highest ratio occurred in July (0.459). The annual mean was 0.434, which is lower than that reported in many previous studies due to drier conditions in the region. During the growth period (April–September), the ratio was 0.438 and this was used in the PEM to estimate aboveground net primary productivity (ANPP). The variation of PAR/SR is largely attributed to differences in sky condition (clearness index) and water vapor in the atmosphere (water vapor pressure). A significant and negative correlation was found between the clearness index and PAR/SR ($r$ = -0.36, $p < 0.05$), while a significant and positive correlation was found between water vapor pressure and PAR/SR ($r$ = 0.48, $p < 0.05$). These findings are consistent with previous studies. This is the first time that PAR/SR, a key input parameter for radiation-based models, has been determined for Mongolia.

Third, to quantify RUE, AGB and above and below-canopy PAR were measured at Bayan Unjuul under different conditions of soil water and air temperature during the growing season of two years. A wide range of RUE (0.23–1.06 g AGB/MJ intercepted

PAR (IPAR)) was found in negative correlation with soil water and low temperature stresses. Compared with the temperature stress, the water stress was a strong down-regulator on RUE, verifying that drought is a major concern for radiation utilization in the study area. The maximum RUE was 2.34±0.16 g AGB/MJ IPAR by excluding the effects of water and temperature stresses, and this was used in the model to estimate ANPP. This is the first study to provide the important model parameter of RUE for natural grassland in Mongolia under various levels of seasonally varying water and temperature conditions.

Fourth, the PEM (using the quantified parameters) was used to estimate pasture productivity at four sites in distinct vegetation zones of Mongolia: Mandalgovi (desert steppe), Bayan Unjuul (dry steppe), Darkhan (steppe), and Bulgan (forest steppe). Simulation results demonstrated that the highest ANPP of 68.2 g carbon (C)/$m^2$ and the lowest ANPP of 6.9 g C/$m^2$ over the growing season (April–September) occurred at Darkhan and Mandalgovi, respectively. Moreover, a comparison of the effect of temperature and water stresses on pasture productivity indicated that water stress was a stronger down-regulator of ANPP. The comparison between measurements and the simulation indicated that simulated ANPP was similar to measured AGB for Mandalgovi and Bayan Unjuul, whereas simulated ANPP tended to overestimate actual AGB for Darkhan and Bulgan.

This thesis represented advances in the field observation and in modeling of pasture productivity in the semi-arid region of Mongolia. This is the first attempt to estimate pasture productivity in the country by applying quantified parameters to the PEM. The model has the advantages of using a simple calculation method which does not require the complex eco-physiological parameters. The model results demonstrate that the parameterized PEM was applicable to dry regions, whereas further model modification is needed for relatively wetter and colder regions.

In the future, advanced technology such as remotely sensed data and Geographical Information Systems should be used alongside this model to represent the spatial distribution of pasture productivity in dry regions. This approach will generate valuable information on feed availability and the efficient management of livestock grazing, which is of great use to herders and decision-makers.

# モンゴル草原における牧草生産力の推定：
# 現地調査およびモデルシミュレーション

## 要約

モンゴルは遊牧民による畜産業の国であり、その経済は畜産物の生産に大きく依存している。自然草地は家畜飼料の主要な供給源であり、草地生産性は大陸性乾燥気候に非常に影響される。草地生産は、土壌水分、気温、太陽光、土壌養分および草地の利用・管理などの多くの要因に左右され、モンゴルでは土壌水分が植物の光利用効率や植生の生産性を決定づける上で最も重要かつ制限的な要因となる。近年、土壌水分において乾燥の傾向が見られ、牧草生育はさらに制限されている。こうした背景から、家畜を維持するために牧草生産力に関して正確かつ時宜に情報を得ることの重要性が浮き彫りとなっている。しかし、モンゴルのような広い国の辺境では、牧草生産力を実測することは困難であると考えられる。したがって、牧草生産力を広範囲にわたって推定できるモデルの開発および妥当性の検証が不可欠である。本論文の主な目的は、砂漠ステップ、乾燥ステップ、ステップおよび森林ステップの牧草生産力を推定するための生産効率モデル（PEM）の入力パラメータ（PAR/SR（太陽放射量に対する光合成有効放射量の割合）および RUE（光エネルギー変換効率））を決定し、その入力パラメータを用いて PEM の適合性を調査することである。

第一に、AGB（地上部バイオマス）と降水量の関係を 15 地点の 1986 年から 2005 年までのデータを用いて解析した結果、AGB は生育期の累積降水量と最も高い有意な相関を示した。月降水量で解析すると、森林ステップの AGB は 6 月の降水量に最も影響を受け、砂漠ステップおよびステップでは 7 月の降水量であった。さらに、砂漠ステップ地域では、降水事象の規模に関わらず、AGB は降水量と強い相関があり、少量（5mm 以下）の降水であっても AGB に影響を与えた。一方、比較的湿潤なステップおよび森林ステップ地域では、AGB は少量の降水では変化せず、比較的多い降水（5.1 mm 以上）によって植物成長が助長された。

これは、降水頻度が高くても少量の降水量では、ステップおよび森林ステップ地域の植生の成長に効果がないことを示唆した。

第二に、バヤンオンジュールの PAR/SR を算出した。月平均の PAR/SR は、4 月および 12 月で最も低く（0.42）、7 月で最も高かった（0.459）。年平均は 0.434 で、研究対象地域が乾燥状態であったため、この数値は過去の大部分の研究に比べ低くかった。生育期（4 月～9 月）の PAR/SR は 0.438 で、この値は後述の PEM シミュレーションで用いられた。PAR/SR のばらつきは、大部分は空の状態（晴天指数）および大気中の水蒸気（水蒸気圧）によるものであった。晴天指数と PAR/SR の間に逆相関（$r$＝-0.36、$p$＜0.05）、水蒸気圧と PAR/SR の間に正相関（$r$＝0.48、$p$＜0.05）が見られ、過去の研究と一致した。

第三に、RUE を定量するために、バヤンオンジュールで 2 年間にわたり、さまざまな土壌水分と気温の条件下で AGB とキャノピー上下の PAR を測定した。土壌水分と低温のストレスによって、広範囲の RUE（0.23～1.06 g AGB/MJ IPAR（遮断される光合成有効放射量））が定量された。低温ストレスに比べ、水分ストレスは RUE に対する強い下方調整要因であり、研究対象地域において干ばつが植物の光利用にとって重要な事象であることが実証された。土壌水分と温度のストレスの影響を除いて計算した結果、最大 RUE は 2.34±0.16 g AGB/MJ IPAR となり、この値は後述の PEM シミュレーションで用いられた。この現地実験は、モンゴルの自然草地で季節を通して変動する土壌水分と気温の条件下で RUE を測定した初めての研究であった。

第四に、PEM を用いて、モンゴル国のマンダルゴビ（砂漠ステップ）、バヤンオンジュール（乾燥ステップ）、ダルハン（ステップ）およびブルガン（森林ステップ）の 4 地点の牧草生産力の推定を行った。シミュレーションの結果、生育期全体（4 月～9 月）の ANPP（地上部の純一次生産力）はダルハンで最も高い 68.2 g C/m$^2$、マンダルゴビで最も低い 6.9 g C/m$^2$ であった。さらに、牧草生産力に及ぼす温度および土壌水分のストレスの影響を比較した結果、水分ストレスが ANPP の強い下方調整要因であることが確証された。マンダルゴビとバヤンオンジュールについては、シミュレーションで算出された ANPP と実測された AGB

が一致したのに対し、ダルハンとブルガンでは、シミュレーション値は実測値を上回る傾向があった。

本論文では、モンゴルの半乾燥地域では初めてとなる PEM モデルのパラメータを定量し、牧草生産力の推定を行った。乾燥した地域（砂漠ステップおよび乾燥ステップ）では PEM による牧草生産力の推定は可能であることが示されたが、比較的湿潤で涼しい地域（ステップおよび森林ステップ）では、なお一層のモデル改良が必要であると結論付けられた。

今後、乾燥した地域の牧草生産力の空間分布を解析するために、リモートセンシングや地理情報システムなどの先端技術を用いて PEM 推定を行うことが必要である。このアプローチにより、遊牧民および政府などの意思決定者に飼料の可用性や効率的な放牧管理に関する情報が提供できると考えられる。

**Appendix B**. A typical view of Mongolian steppe (in Bayan Unjuul, Mongolia)

**Appendix C.** Plant species present in Bayan Unjuul, Mongolia

***Stipa Krylovii***

***Agropyron cristatum***

***Cleistogenes squarrosa***

***Elymus chinensis***

***Carex korshinskii***

**Appendix C.** continued

***Artemisia adamsii***

***Salsola collina***

***Chenopodium*** species dominated field

***Caragana stenophylla***


***Caragana microphylla***

**Appendix C.** continue*d*

***Potentilla bifurca***

***Potentilla multifida***

***Dontostemon* spp.**

***Sibbaldianthe adepressa***

***Poa attenuate***

***Allium mongolicum*.**

***Convolvulus ammanii***

**Appendix D.** Visible differences in plant growth between the water treatments and between the two years (photos taken on 8 Aug 2009 and 19 Aug 2010, respectively).

Control plot in 2009

Control plot in 2010

Low-irrigation plot in 2009

Low-irrigation plot in 2010

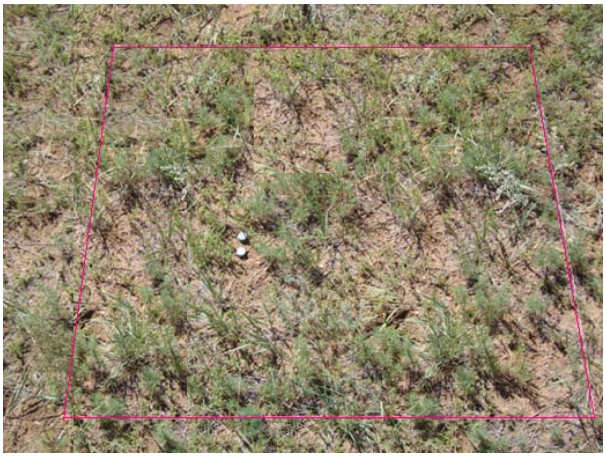

High-irrigation plot in 2009

High-irrigation plot in 2010

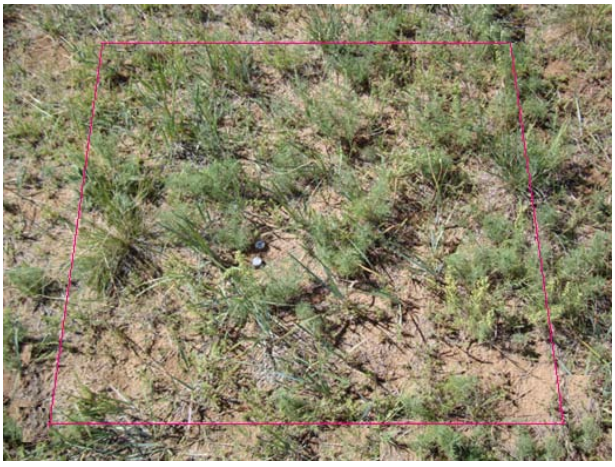

# REFERENCES


Akmal M, Janssens MJJ. 2004. Productivity and light use efficiency of perennial ryegrass with contrasting water and nitrogen supplies. Field Crop Res. 88:143–155.

Alados I, Foyo-Moreno I, Alados-Arboledas L. 1996. Photosynthetically active radiation: Measurements and modelling. Agric For Meteorol 78:121–131.

Allen RG, Pereira LS, Raes D, Smith M. 1998. Crop evapotranspiration-Guidelines for computing crop water requirements. Rome, Italy: FAO Irrigation and Drainage. 56:161–169.

Andrade FH, Uhart SA, Arguissain GG, and Ruiz RA. 1992. Radiation use efficiency of maize grown in a cool area. Field Crop Res. 28:345–354.

Aschan G, Pfanz H. 2003. Non-foliar photosynthesis – a strategy of additional carbon acquisition. Flora. 198:81–97.

Asrar G, Fuchs M, Kanemasu ET, Hatfield JL. 1984. Estimating absorbed photosynthetic radiation and leaf area index from spectral reflectance in wheat. Agron J. 76:300–306.

Batima P. 2006. Climate Change Vulnerability and Adaptation in the Livestock Sector of Mongolia. A Final Report Submitted to Assessments of Impacts and Adaptations to Climate Change (AIACC), Project No. AS 06.

Batima P, Dagvadorj D. 2000. Climate Change and Its Impact in Mongolia. JEMR Publishing. Ulaanbaatar. pp.46–93.

Bat-Oyun T, Shinoda M, Tsubo M. 2010. Estimation of pasture productivity in Mongolian grasslands: field survey and model simulation. J Agric Meteorol. 66 (1):31–39.

Bat-Oyun T, Shinoda M, Tsubo M. 2011. Effects of water and temperature stresses on radiation use efficiency in a semi-arid grassland. doi: 10. 1080/17429145. 2011.564736.

Bell MJ, Wright GC, Hammer GL. 1992. Night temperature affects radiation-use efficiency in peanut. Crop Sci. 32:1329–1335.

Blanke MM, Lenz F. 1989. Fruit photosynthesis – a review. Plant Cell Environ. 12:31–46.

Blum A. 1996. Crops response to drought and the interpretation of adaptation. Plant Growth Regul. 20:135–148.

Bolortsetseg B, Erdenetsetseg B, Bat-Oyun Ts. 2002. Impact of past 40 years climate change on pasture plant phenology and production. Papers in Meteorology and Hydrology of Mongolia. 24:108–114.

Bolortsetseg B. 2006. Climate change Vulnerability and Adaptation in the Livestock Sector of Mongolia. Assessments of Impacts and Adaptations to Climate Change (AIACC) final report. Ulaanbaatar, 44 pp.

Britton CM, Dodd JD. 1976. Relationships of photosynthetically active radiation and shortwave irradiance. Agric Meteorol 17:1–7.

Chen Y, Lee G, Lee P, Oikawa T. 2007. Model analysis of grazing effect on above-ground biomass and above-ground net primary production of a Mongolian grassland ecosystem. J Hydrol. 333:155–164.

Chuluun T, Ojima D. 2002. Land use change and carbon cycle in arid and semi-arid lands of East and Central Asia Sci China. 45:48–54.

Coleman DC. 1976. A review of root production processes and their influence on soil biota in terrestrial ecosystems. In “The Role of Terrestrial and Aquatic Organisms in Decomposition Processes”. Oxford, England: Blackwell Scientific Publications. pp 417–434.

Comstock J, Ehleringer J. 1993. Stomatal response to humidity in common bean (*Phaseolus vulgaris* L.): implications for maximum transpiration rate, water-use efficiency and productivity. Aust J Plant Physiol. 20:669–691.

Cooper JP. 1975. Photosynthesis and Productivity in Different Environments. IBP Vol. 3. Cambridge University Press, Cambridge.

Correia MJ, Rodrigues ML, Osório ML, Chaves MM. 1999. Effects of growth temperature on the response of lupin stomata to drought and abscisic acid. Aust J Plant Physiol. 26:549–559.

Coupland RT. 1979. Grassland Ecosystems of the World. IBP Vol. 18. Cambridge University Press

Dai A, Trenberth KE, Karl T. 1998. Global variations in droughts and wet spells: 1900–1995. Geophysical Research Letters. 25:3367–3370.

Day W, Lawlor DW, Legg BJ. 1981. The effect of drought on barley: soil and plant water relations. J Agric Sci. 96:61–77.

Devlin RM, Barker AV. 1971. Photosynthesis. New York: Univ. of Massachusetts.

Easterling DR, Evans JL, Groisman PYa, Karl TR, Kunkel KE, Ambenje P. 2000. Observed variability and trends in extreme climate events: A brief review. Bull Amer Meteor Soc. 81:417–425.

Fang J, Piao S, Zhou L, He J, Wei F, Myneni RB, Tucker CJ, Tan K. 2005. Precipitation patterns alter growth of temperate vegetation. Geophys Res Lett., 32, L21411, doi:10.1029/2005GL024231.

Farquhar GD, von Caemmerer S, Berry JA. 1980. A biochemical model of photosynthetic $CO_2$ assimilation in leaves of C3 species. Planta. 149:78–90.

Fay P, Carlisle AJD, Knapp AK, Blair JM, Collins SL. 2003. Productivity responses to altered rainfall patterns in a C4-dominated grassland. Oecologia. 137:245–251.

Fernandez-Gimenez ME, Allen-Diaz B. 1999. Testing a non-equilibrium model of rangeland vegetation dynamics in Mongolia. J Appl Ecol. 36:871–885.

Field CB. 1995. Global net primary production: combining ecology and remote sensing.

Remote Sens Environ. 51:74–88.

Finch DA, Bailey WG, McArthur LJB, Nasitwitwi M. 2004. Photosynthetically active radiation regimes in a southern African savanna environment. Agric For Meteorol. 122:229–238.

Frouin R, Pinker RT. 1995. Estimating photosynthetically active radiation (PAR) at the earth's surface from satellite observations. Remote Sens Environ. 51:98–107.

Gallo KP, Daughtry CST. 1986. Techniques for measuring intercepted and absorbed photosynthetically active radiation in corn canopies. Agron J. 78:752–756.

Goward SN, Huemmrich KF. 1992. Vegetation canopy PAR absorptance and the normalized difference vegetation index: An assessment using the SAIL model. Remote Sens Environ. 39:119–140.

Gower ST, Kucharik CJ, Norman JM. 1999. Direct and indirect estimation of leaf area index, fAPAR, and net primary production of terrestrial ecosystems. Remote Sens Environ. 70: 29–51.

Gunin PD, Vostokova EA, Dorofeyuk NI, Tarsov PE, Black CC. 1999. Natural and anthropogenic factors and the dynamics of vegetation distribution. In Vegetation dynamics of Mongolia (ed by Werger, M. J. A.). Geobotany 26. Kluwer Academic Publishers. AH Dordrecht. Netherlands. pp7–43.

Hanan NP, Prince SD, Bégué A. 1995. Estimation of absorbed photosynthetically active radiation and vegetation net production efficiency using satellite data. Agric For Meteorol. 76:259–276.

Hansen V. 1984. Spectral distribution of solar radiation on clear days: A comparison between measurements and model estimates. J Climate Appl Meteorol 23:772–780.

Hew CS, Ng YW, Wong SC, Yeoh HH, Ho KK. 1984. Carbon dioxide fixation in orchid aerial roots. Physiol. Plant. 60:154–158.

Howell TA, Meek DW, Hatfield JL. 1983. Relationship of photosynthetically active radiation to shortwave radiation in the San Joaquin valley. Agric Meteorol 28:157–175.

Hu B, Wang Y, Liu G. 2007. Measurements and estimations of photosynthetically active radiation in Beijing. Atmospheric Research. 85:361–371.

Hunt JE, Kelliher FM, McSeveny TM, Byers JT. 2002. Evaporation and carbon dioxide exchange between the atmosphere and a tussock grassland during a summer drought. Agric For Meteorol. 111:65–82.

Jeuffroy MH, Ney B. 1997. Crop physiology and productivity. Field Crop Res. 53:3–16.

Johnson D, Sheehy D, Miller, D, Damiran, D. 2006. Mongolian rangelands in transition. Sécheresse. 17 (1–2): 133–141.

Jones HG. 1992. Plants and Microclimate: A Quantitative Approach to Environmental Plant Physiology. Cambridge, UK: Cambridge University Press.

Jordan CF. 1981. Tropical Ecology. Hutchinson Ross, Stroudsberg

Knapp AK, Smith MD. 2001. Variation among biomes in temporal dynamics of aboveground primary production. Science. 291:481–484.

Kondoh A, Kaihotsu I. 2003. Preliminary analysis on the relationship between vegetation activity and climatic variation in Mongolia (in Japanese). Journal of Arid Land Studies 13(2): 147–151.

Kramer PJ. 1983. Water relations of plants. New York: Academic Press. 489 p.

Larcher W. 2003. Physiological Plant Ecology, 4th ed. Berlin: Springer-Verlag.

Lauenroth WK, Sala OE. 1992. Long term forage production of North American shortgrass steppe. Ecol Appl. 2:397–403.

Li SG, Eugster W, Asanuma J, Kotani A, Davaa G, Oyunbaatar D, Sugita M. 2008. Response of gross ecosystem productivity, light use efficiency and water use

efficiency of Mongolian steppe to seasonal variations in soil moisture. J Geophys Res. 113: G01019. doi: 10.1029/2006JG000349.

Lobell DB, Hicke JA, Asner GP, Field CB, Tucker CJ, Los O. 2002. Satellite estimates of productivity and light use efficiency in United States agriculture, 1982–98. Glob Change Biol. 8:722–735.

McCree KJ. 1966. A solarimeter for measuring photosynthetically active radiation. Agric Meteorol 3:353–366.

Miyazaki S, Yasunari T, Miyamoto T, Kaihotsu I, Davaa G, Oyunbaatar D, Natsagdorj L, Oki T. 2004. Agrometeorological conditions of grassland vegetation in central Mongolia and their impact for leaf area growth. J Geophys Res. 109: D22106.

Mongolian statistical yearbook 2009, by National Statistical Office, source: **http://www.nso.mn**

Monneveux P, Pastenes C, Reynolds MP. 2003. Limitations to photosynthesis under light and heat stress in three high-yielding wheat genotypes. J Plant Physiol. 160:657–666.

Monsi M, Saeki T. 1953. Über den Lichtfaktor in den Pflanzengesellschaften und seine Bedeutung für die Stoffproduktion. Jap J Bot. 14:22–52.

Monteith JL, Unsworth M. 1990. Principles of environmental physics, 2nd edn. London: Edward Arnold. pp. 291.

Monteith JL. 1972. Solar radiation and productivity in tropical ecosystems. J Appl Ecol. 9:747–766.

Monteith JL. 1973. Principles of Environmental Physics. Edward Arnold, London.23-38.

Monteith JL. 1977. Climate and efficiency of crop production in Britain. Philos Trans R Soc B-Biol Sci. 281:271–294.

Moon P. 1940. Proposed standard solar-radiation curves for engineering use. J Franklin

Inst 230:583–618.

Mougin E, Lo Seen D, Rambal S, Gaston A, Hiernaux P. 1995. A regional Sahelian grassland model to be coupled with multispectral satellite data: I. Model description and validation. Remote Sens Environ. 52:181–193.

Munkhtsetseg E, Kimura R, Wang J, Shinoda M. 2007. Pasture yield response to precipitation and high temperature in Mongolia. J Arid Environ. 70:94–110.

Nachinshonhor GU. 2001. Influence of climate and nomadic activities on the plant community of Mongolian grasslands. PhD thesis. 207p.

Nakano T, Nemoto M, Shinoda M. 2008. Environmental controls on photosynthetic production and ecosystem respiration in semi-arid grasslands of Mongolia. Agric For Meteorol. 148:1456–1466.

Nandintsesteg B, Shinoda M. 2010. Seasonal change of soil moisture in Mongolia: its climatology and modeling. Int J Climatol. doi: 10.1002/joc.2134.

Natsagdorj L. 2009. Desertification and Climate Change. Ulaanbaatar: Benbi san publishing.

Ni J. 2003. Plant functional types and climate along a precipitation gradient in temperate grasslands, north-east China and south-east Mongolia. J Arid Environ. 53: 501–516.

Nilsen ET. 1995. Stem photosynthesis extent, patterns and role in plant carbon economy, in: Gartner, B. (Ed.), Plant stems – Physiology and functional morphology, Academic Press., San Diego, pp. 223–240.

Nippert JB, Knapp AK, Blair JM. 2006. Intra-annual rainfall variability and grassland productivity: Can the past predict the future?. Plant Ecol. 184:65–74.

Nouvellon Y, Seen DL, Rambal S, Bégué A, Moran MS, Kerr Y, Qi JG. 2000. Time course of radiation use efficiency in a shortgrass ecosystem: Consequences for

remotely sensed estimation of primary production. Remote Sens Environ. 71:43–55.

Noy-Meir I. 1973. Desert ecosystems: environment and producers. Annu Rev Ecol Syst. 4:25–51.

Papaioannou G, Nikolidakis G, Asimakopoulos D, Retalis D. 1996. Photosynthetically active radiation in Athens. Agric Forest Meteorol 81:287–298.

Papaioannou G, Papanikolaou N, Retalis D. 1993. Relationships of photosynthetically active radiation and shortwave irradiance. Theor Appl Climatol. 48:23–27.

Paruelo JM, Epstein HE, Lauenroth WK, Burke IC. 1997. ANPP estimates from NDVI for the central grassland region of the United States. Ecology. 78:953–958.

Pastenes C, Horton P. 1996. Effect of high temperature on photosynthesis in beans — II: $CO_2$ assimilation and metabolite contents. Plant Physiol. 112:1253–1260.

Pinker RT, Laszlo I. 1992. Global distribution of photosynthetically active radiation as observed from satellites. J Climate. 5:56–65.

Potter CS, Klooster S, Brooks V. 1999. Interannual variability in terrestrial net primary production: Explorations of trends and controls on regional to global scales. Ecosystems. 2:36–48.

Potter CS, Randerson JT, Field CB, Matson PA, Vitousek PM, Mooney HA, Klooster SA. 1993. Terrestrial ecosystem production: a process model based on global satellite and surface data. Global Biogeochem Cy. 7:811–841.

Prince SD, Goward SJ. 1995. Global primary production: a remote sensing approach. J Biogeogr. 22:815–835.

Raich JW, Rastetter EB, Mellilo JM, Kicklighter, DW, Steudler PA, Peterson BJ. 1991. Potential net primary productivity in South America: Application of a global model. Ecol Appl. 1:399–429.

Rao CR. 1984. Photosynthetically active components of global solar radiation: Measurements and model computations. Arch Meteorol Geophys Bioclim Ser B 34:353–364.

Roberts MJ, Long SP, Tieszen LL, Beadle CL. 1985. Measurement of plant biomass and net primary production. In Techniques in Bioproductivity and Photosynthesis, 2nd edition. Eds. J Coombs, D O Hall, S P Long and J M O Scurlock. Pergamon Press, Oxford, pp. 1–19.

Rodskjer N. 1983. Spectral daily insolation at Uppsala, Sweden. Arch Meteorol Geophys Bioclim Ser B 33:89–98.

Ross J, Sulev M. 2000. Sources of errors in measurements of PAR. Agric For Meteorol. 100: 103–125.

Runyon J, Waring RH, Goward SN, Welles JM. 1993. Environmental limits on net primary production and light-use efficiency across the Oregon transect. Ecol Appl. 4:226–237.

Russell G, Jarvis PG, Monteith JL. 1989. Absorption of radiation by canopies and stand growth. In ‘Plant Canopies: Their Growth, Form and Function’. Cambridge, UK: Cambridge University Press. pp 21–39.

Sala OE, Lauenroth WK. 1982. Small rainfall events: an ecological role in semiarid regions. Oecologia (Berlin). 53:301–304.

Sellers PJ. 1987. Canopy reflectance, photosynthesis, and transpiration. II. The role of biophysics in the linearity of their interdependence. Remote Sens Environ. 21:143–183.

Sellers PJ, Berry JA, Collatz GJ, Field CB, Hall FG. 1992. Canopy reflectance, photosynthesis and transpiration, III, A reanalysis using improved leaf models and new canopy integration scheme. Remote Sens Environ. 42:187–216.

Shinoda M, Ito S, Nachinshonhor GU, Erdenetsetseg D. 2007. Phenology of Mongolian grasslands and moisture conditions. J Meteor Soc Japan. 85 (3):359–367.

Shinoda M, Kimura R, Mikami M, Tsubo M, Nishihara E, Ishizuka M, Yamada Y, Munkhtsetseg E, Jugder D, Kurosaki Y. 2010a. Characteristics of dust emission in the Mongolian steppe during the 2008 DUVEX intensive observational period. SOLA. 6:9–12.

Shinoda M, Nachinshonhor GU, Nemoto M. 2010b. Impact of drought on vegetation dynamics of the Mongolian steppe: A field experiment. J Arid Environ. 74:63–69.

Sinclair TR, Gardner FP. 1998. Principles of ecology in plant production. Wallingford: CAB International. pp. 189.

Sinclair TR, Muchow RC. 1999. **Radiation use efficiency**. Adv Agron. 65:215–265.

Suzuki R, Masuda K, Dye DG. 2007. Interannual covariability between actual evapotranspiration and PAL and GIMMS NDVIs of northern Asia. Remote Sens Environ. 106:387–398.

Tao F, Yokozawa M, Zhang Z, Xu Y, Hayashi Y. 2005. Remote sensing of crop production in China by production efficiency models: models comparisons, estimates and uncertainties. Ecol Model. 183:385–396.

Tesfaye K, Walker S, Tsubo M. 2006. Radiation interception and radiation use efficiency of three grain legumes under water deficit conditions in a semi-arid environment. Eur J Agron. 25:60–70.

Tsubo M, Walker S. 2005. Relationships between photosynthetically active radiation and clearness index at Bloemfontein, South Africa. Theoretical and Applied Climatology 80:17–25.

Tugjsuren N, Takamura T. 2001. Investigation for Photosynthetically Active Radiation Regime in the Mongolian Grain Farm Region. 57 (4):201–207.

Udo SO, Aro TO. 1999. Global PAR related to global solar radiation for central Nigeria. Agric For Meteorol 97:21–31.

UNEP. 1992. World Atlas of Desertification. London:

Wang Q, Kakubari Y, Kubota M, Tenhunen J. 2007. Variation of PAR to global solar radiation ratio along altitude gradient in Naeba Mountain. Theoretical and Applied Climatology. 87:239–253.

Weiss D, Schönfeld M, Halevy AH. 1988. Photosynthetic activities in the Petunia corolla. Plant Physiol. 87:666–670.

Weltzin JF, Loik ME, Schwinning S, Williams DG, Fay PA, Haddad BM, Harte J, Huxman TE, Knapp AK, Lin G, Pockman WT, Shaw MR, Small EE, Smith MD, Smith SD, Tissue DT, Zak JC. 2003. Assessing the response of terrestrial ecosystems to potential changes in precipitation. BioScience. 53:941– 952.

Willmott CJ. 1982. Some comments on the evaluation of model performance. Bull Am Meteorol Soc. 63:1309–1313.

Wilson JB. 1988. A review of evidence on the control of shoot: root ratio, in relation to models. Ann Bot. 61 (4):433–449.

Yamaguchi Y, Shinoda M. 2002. Soil moisture modeling based on multiyear observations in the Sahel. J Appl Meteorol. 41: 1140–1146. doi: 10.1175/1520–0450(2002)041.

Yuan J, Niu Z, Wang C. 2006. Vegetation NPP Distribution Based on MODIS Data and CASA Model – A Case Study of Northern Hebei Province. Chin Geogr Sci. 16(4): 334–341.

Yunatov AA. 1976. Fundamental Characteristics of the Vegetation of Mongolian People's Republic. Ulaanbaatar: Mongolian Academy of Science.

Zhang X, Zhang Y, Zhoub Y. 2000. Measuring and modeling photosynthetically active radiation in Tibet Plateau during April–October. Agric Forest Meteorol 102:207–

212

Золотокрылин АН. 2001. Климатическое опустынивание - Автореферат на соискание уч.ст.д-ра. геогр. наук. М, с48.

# LIST OF PUBLICATIONS

Tserenpurev BAT-OYUN, Masato SHINODA, and Mitsuru TSUBO. 2010. Estimation of pasture productivity in Mongolian grasslands: field survey and model simulation. Journal of Agricultural Meteorology, 66 (1): 31–39, (Chapter 5).

Tserenpurev Bat-Oyun, Masato Shinoda and Mitsuru Tsubo. 2011. Effects of water and temperature stresses on radiation use efficiency in a semi-arid grassland, Journal of Plant Interactions, DOI: 10.1080/17429145.2011.564736, (Chapter 4).